Microglia contribute to methamphetamine reinforcement and reflect persistent transcriptional and morphological adaptations to the drug

Samara J. Vilca[1,2†], Alexander V. Margetts[1-3†], Isabella Fleites[1-3], Claes Wahlestedt[1-3] & Luis M. Tuesta[1-3*]

GRAPHICAL ABSTRACT

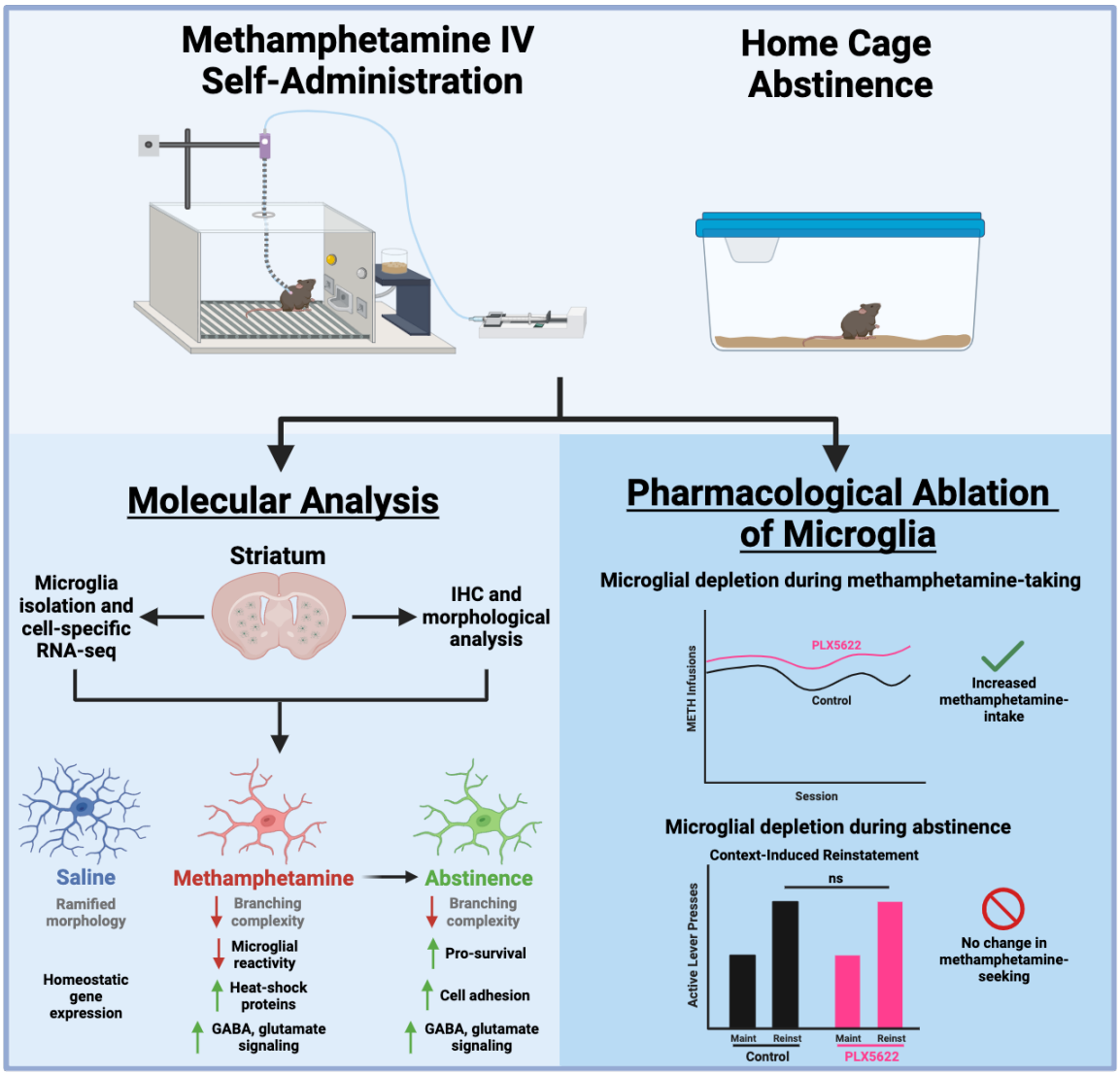

Microglia contribute to methamphetamine reinforcement and reflect persistent transcriptional and morphological adaptations to the drug

Samara J. Vilca[1,2†], Alexander V. Margetts[1-3†], Isabella Fleites[1-3], Claes Wahlestedt[1-3] & Luis M. Tuesta[1-3*]

[1] Department of Psychiatry & Behavioral Sciences
[2] Center for Therapeutic Innovation
[3] Sylvester Comprehensive Cancer Center
University of Miami Miller School of Medicine, Miami, FL 33136
[†] Denotes equal contribution
* Corresponding author (ltuesta@miami.edu)

Abstract

Methamphetamine use disorder (MUD) is a chronic, relapsing disease that is characterized by repeated drug use despite negative consequences and for which there are currently no FDA approved cessation therapeutics. Repeated methamphetamine (METH) use induces long-term gene expression changes in brain regions associated with reward processing and drug-seeking behavior, and recent evidence suggests that methamphetamine-induced neuroinflammation may also shape behavioral and molecular responses to the drug. Microglia, the resident immune cells in the brain, are principal drivers of neuroinflammatory responses and contribute to the pathophysiology of substance use disorders. Here, we investigated transcriptional and morphological changes in striatal microglia in response to methamphetamine-taking and during methamphetamine abstinence, as well as their functional contribution to drug-taking behavior. We show that methamphetamine self-administration induces transcriptional changes related to protein folding, mRNA processing, immune signaling, and neurotransmission in striatal microglia. Importantly, many of these transcriptional changes persist through abstinence, a finding supported by morphological analysis. Functionally, we report that microglial ablation increases methamphetamine-taking, possibly involving neuroimmune and neurotransmitter regulation. In contrast, microglial depletion did not alter methamphetamine-seeking behavior following 21 days of abstinence, highlighting the complexity of drug-seeking behaviors. Taken together, these results suggest that methamphetamine induces both short and long-term changes in striatal microglia that contribute to altered drug-taking behavior and may be leveraged for preclinical development of methamphetamine cessation therapeutics.

1. Introduction

Methamphetamine use disorder (MUD) is a chronic, relapsing disease that is estimated to cost the United States upwards of $24 billion annually (Nicosia, Pacula et al. 2009). Within the past decade, the number of individuals with MUD increased by 37%, while deaths attributed to methamphetamine overdose more than doubled (CDC 2021). Methamphetamine has a high potential for addiction due to its potent activation of the brain reward system (Chang, Alicata et al. 2007). Indeed, users can experience intense euphoria, increased energy, and alertness (Cruickshank and Dyer 2009). At higher doses, methamphetamine causes hyperthermia as well as other aversive effects such as arrhythmia, insomnia, paranoia, aggression, and psychosis (Barr, Panenka et al. 2006, Gonzales, Mooney et al. 2010). Methamphetamine reward and reinforcement is attributed to increased dopamine signaling by neurons of the mesocortical, mesolimbic, and nigrostriatal pathways (Everitt and Robbins 2005, Cruickshank and Dyer 2009). Although these neural mechanisms are well characterized, there are currently no FDA approved medications for the treatment of MUD (Karila, Weinstein et al. 2010).

Microglia are the resident immune cell of the central nervous system and have various roles throughout the lifespan including neuronal development and synaptic pruning (Paolicelli, Bolasco et al. 2011), surveillance of the neural environment and circuit formation (Parkhurst, Yang et al. 2013, Wake, Moorhouse et al. 2013), and aging and disease (Keren-Shaul, Spinrad et al. 2017, Salter and Stevens 2017). Accumulating evidence suggests that microglia can respond to methamphetamine exposure (LaVoie, Card et al. 2004, Sekine, Ouchi et al. 2008, Kitamura, Takeichi et al. 2010). For instance, methamphetamine can directly bind several immune receptors expressed in microglia such as TLR4 (Wang, Northcutt et al. 2019) and sigma-1 (Chao, Zhang et al. 2017). Additionally, microglia can respond to methamphetamine-induced neuronal activity and signaling from other glia (LaVoie, Card et al. 2004, Kuhn, Francescutti-Verbeem et al. 2006, Canedo, Portugal et al. 2021). Microglia then release various cytokines which can further amplify the neurotoxic and inflammatory effects of methamphetamine (Krasnova, Justinova et al. 2016). Specifically, striatal microglia have been shown to exhibit a unique transcriptional profiles at baseline (Ayata, Badimon et al. 2018), and after exposure to methamphetamine (Thanos, Kim et al. 2016, Kays and Yamamoto 2019). However, the transcriptional response of microglia to methamphetamine, and particularly prolonged abstinence, have yet to be examined using a clinically relevant animal model of MUD.

Given the evidence suggesting that microglia are actively engaged in the molecular response to methamphetamine, we hypothesized that transcriptional and morphological responses would be more persistent using a clinically relevant model of methamphetamine reinforcement, and that microglia would play a functional role in active methamphetamine-taking. We thus established a model of methamphetamine intravenous self-administration (METH IVSA) in mice as well as a computational pipeline to profile these changes and test the role of microglia in methamphetamine-taking and -seeking following prolonged abstinence.

2. Methods

2.1. Animals

Male C57BL/6J mice (9 weeks old ~25-30 g; Jackson Laboratories, Bar Harbor, ME; SN: 000664) were housed in the animal facilities at the University of Miami Miller School of Medicine. Mice were maintained on a 12:12 h light/dark cycle (0600 hours lights on; 1800 hours lights off) and were housed 3 to 5 per cage. Animals were provided with food and water *ad libitum*. Mice representing each experimental group were evenly distributed among testing sessions. All animals were maintained according to the National Institutes of Health guidelines in Association for Assessment and Accreditation of Laboratory Animal Care accredited facilities. All experimental protocols were approved by the Institutional Animal Care and Use Committee at the University of Miami Miller School of Medicine. Whenever possible, the experimenter was blind to the experimental and/or treatment group.

2.2. Drugs

For self-administration experiments in mice, methamphetamine hydrochloride (NIDA Drug Supply Program, Research Triangle Park, NC, USA) was dissolved in 0.9% sterile saline.

2.3. Microglial Depletion

To deplete microglia during METH IVSA, CSF1R inhibitor PLX5622 was formulated in AIN-76A chow (1200 ppm; Research Diets, New Brunswick, NJ, USA). PLX5622 has been shown to ablate nearly all microglia (99%) when administered for at least 5 days (Spangenberg, Severson et al. 2019). To determine the effect of microglia depletion on methamphetamine-taking, mice were treated with PLX5622 5 days prior to starting METH IVSA, and for the duration of Acquisition and Maintenance. To determine the effect of microglia depletion on methamphetamine-seeking, mice were treated with PLX5622 beginning after the last maintenance session and for the duration of forced home cage abstinence.

2.4. Jugular Catheter Surgery

Mice were anesthetized with an isoflurane (1–3%)/oxygen vapor mixture and implanted with an indwelling jugular catheter. Briefly, the catheter consisted of a 6.5-cm length of Silastic tubing fitted to a guide cannula (PlasticsOne, Protech International Inc., Boerne, TX, USA) bent at a curved right angle and encased in dental acrylic resin and silicone. The catheter tubing was passed subcutaneously from the animal's back to the right jugular vein, and 1-cm length of the catheter tip was inserted into the vein and anchored with surgical silk sutures. Mice were administered Meloxicam (5 mg/kg) subcutaneously prior to start of surgery and 24 hours post-surgery. Catheters were flushed daily with physiological sterile saline solution (0.9% w/v) containing heparin (10–60 USP units/mL) beginning 48 hours after surgery. Animals were allowed 3-5 days to recover from surgery before commencing METH IVSA. Catheter integrity was tested with the ultra-short-acting barbiturate anesthetic Brevital (methohexital sodium, Eli Lilly, Indianapolis, IN, USA).

2.5. Operant IV Self-Administration Training

Mice were permitted to self-administer methamphetamine or saline intravenous infusions during daily 2-hr sessions. Infusions were delivered through Tygon catheter tubing (Braintree Scientific, MA, USA) into the

intravenous catheter by a variable speed syringe pump (Med Associates Inc, Fairfax, VT, USA). Self-administration sessions were carried out in operant chambers containing 2 retractable levers (1 active, 1 inactive) and a yellow cue light located above the active lever which illuminated during the intravenous infusion as well as during the 20 s post-infusion time out (TO). During Acquisition, mice started on a fixed ratio 1 (FR1) schedule of reinforcement for infusions 1 to 5, then FR2 for infusions 6 to 10, and FR3 for the remainder of the session. Completion of the response criteria on the active lever resulted in the delivery of an intravenous infusion (14 μL over 2 sec) of methamphetamine (0.05 mg/kg/infusion) or 0.9% saline. Responses on the inactive lever were recorded but had no scheduled consequences. After 5 consecutive days of Acquisition, mice were allowed to self-administer methamphetamine or saline during 10 consecutive daily 2-hr Maintenance sessions. Animals that did not demonstrate stable responding (less than 7 infusions per 2-hr session) or showed signs of compromised catheter patency were excluded from analysis.

2.6. Forced Home Cage Abstinence and Reinstatement

After 15 days of methamphetamine self-administration (Acquisition and Maintenance), mice underwent 21 days of forced home cage abstinence. A context-induced reinstatement session was then conducted on Day 21, where completion of response criteria resulted in the presentation of the light stimulus previously paired with methamphetamine or saline infusion delivery; however, no reward was delivered. Active lever presses were recorded and interpreted as a measure of drug-seeking.

2.7. Microglial Isolation

Mice were anesthetized with isoflurane and perfused through the ascending aorta with 0.1 M phosphate buffer saline (PBS pH 7.4, Gibco, Waltham, MA, USA) plus heparin (7,500 USP units). Tissues were dissected and transported in Hibernate A Medium (Gibco) before dissociation. Briefly, tissue was enzymatically and mechanically dissociated, and debris removed using the Adult Brain Dissociation Kit (Miltenyi Biotec, Bergisch Gladbach, Germany). The resulting single cell suspension was incubated with anti-mouse CD11b (i.e., microglia-specific) magnetic MicroBeads (Miltenyi Biotec, #130–093–634) and microglia were positively selected for via column purification (Miltentyi Biotec, #130-042-201).

2.8. Brain Perfusion and Fixation

Mice were anesthetized with isoflurane and perfused through the ascending aorta with PBS pH 7.4 (Gibco) plus heparin (7,500 USP units), followed by fixation with 4% paraformaldehyde in PBS. Brains were collected and postfixed overnight in 4% paraformaldehyde, then transferred to 30% sucrose with 0.05% sodium azide (S2002, Sigma-Aldrich, St. Louis, MO, USA) in PBS for 72 hrs. All brains were cut into 35 μm coronal sections on a Leica CM1900 cryostat and placed into 12-well plates containing PBS with 0.02% sodium azide at 4°C until processing for immunohistochemistry.

2.9. Fluorescence Immunolabeling

Floating sections were processed for fluorescent immunostaining of microglia. Sections were rinsed in PBS and then blocked for 1 hour in Blocking Buffer consisting of 10% normal donkey serum (017-000-121, Jackson ImmunoResearch), 0.5% Triton X-100 (T8787, Sigma), and PBS. Thereafter, sections were incubated in primary antibody diluted in Blocking Buffer overnight at 4°C. The primary antibody used was rabbit anti-Iba1 (1:1000, 019-19741, Wako Fujifilm). On day 2, sections were washed in PBS three times for 5 min each, then incubated with the following secondary antibody: Alexa Fluor 488 donkey anti-rabbit (1:500, A-21206, Invitrogen). Sections were incubated with secondary antibodies in PBS with 2% normal donkey serum for 2 hours at room temperature in the dark. Next, sections were rinsed in PBS three times for 5 min each and mounted on slides with ProLong Diamond Antifade Mountant with DAPI (P36962, Invitrogen) and coverslipped. Fluorescent images were acquired on an ECHO Revolve microscope using a 20X objective. All antibodies used have been previously validated for the intended applications, as per manufacturer. For all representative images of qualitative data, the immunolabeling experiment was successfully repeated in 4 animals.

2.10. Sholl Analysis

Acquired images were converted to 8-bit grayscale and analyzed using FIJI (Schindelin, Arganda-Carreras et al. 2012). Iba1 positive channel was enhanced across the entire image, followed by noise de-speckling. The image was then converted to binary and skeletonized. Microglia morphology was analyzed using Sholl Analysis plugin (Ferreira, Blackman et al. 2014). Each condition consisted of 40-43 counted microglia (10-12 microglia per animal) from a total of 4 animals.

2.11. RNA-Sequencing

Isolated microglia were centrifuged for 5 min at 600xg and resuspended in RLT plus buffer (Qiagen) for extraction and purification of total RNA. RNA input was normalized and NGS libraries were prepared using NEBNext Single Cell/Low Input RNA Library Prep Kit for Illumina (New England BioLabs) according to the manufacturer's instructions. Paired-end 100 bp sequencing was performed on a NovaSeq6000 sequencer (Illumina). All RNA-seq data used in this study were mapped to the mm10 genome. Prior to mapping, raw RNA-seq datasets were trimmed using Trimgalore (v.0.6.7) and cutadapt (v.1.18). Illumina sequence adaptors were removed and the leading and tailing low-quality base-pairs were trimmed following default parameters. Next, pair-end reads were mapped to the genome using STAR (v.2.7.10a) with the following parameters: –outSAMtype BAM SortedByCoordinate –outSAMunmapped Within –outFilterType BySJout –outSAMattributes NH HI AS NM MD XS –outFilterMultimapNmax 20 –outFilterMismatchNoverLmax 0.3 --quantMode TranscriptomeSAM GeneCounts. The resulting bam files were then passed to StringTie (v.2.1.5) to assemble sequenced alignments into estimated transcript and gene count abundance given the NCBI RefSeq GRCm38 (mm10) transcriptome assembly.

2.12. Differential Gene Expression Analysis

The R/Bioconductor DESeq2 package (v.1.38.3) was used to detect the differentially expressed genes in microglia throughout different phases. Following filtering for low count genes and outliers, as determined by DESeq2 and Cook's distance, only genes with an adjusted p-value < 0.05 were considered as significantly differentially expressed. In the case where biological replicates showed great variability indicating outliers, a supervised removal of such replicates from each group was conducted (**Supplementary Fig. 1**).

2.13. Functional Enrichment Analysis

The enrichGO function from the R/Bioconductor clusterProfiler package (v.4.6.2) was used to perform gene ontology (GO) enrichment analysis. Only significantly differentially expressed genes with an adjusted p-value < 0.05 and lfcSE ≤ 1.5 were included. Resulting GO terms and pathways with an FDR < 0.05 were considered after using a custom background from all genes that were expressed after DESeq2 adjustment. The associated GO and pathway enrichment plots were generated using the ggplot2 package. Heatmaps were generated using the R/Bioconductor package pheatmap (v.1.0.12) of regularized log (rlog) transformed normalized counts. All the other plots were generated using the ggplot2 package (v.3.4.2) with labels added using Adobe Illustrator for clarity.

2.14. Statistical analyses

Animal sample size was justified by previously published data or preliminary experiments. Data distribution was assumed to be normal. All animals were randomly assigned to treatment groups. For self-administration experiments, animals that did not achieve stable levels of intake (<20% variation in intake across three consecutive days) or that took fewer than 7 methamphetamine infusions on average across sessions were excluded from data analysis. All data were analyzed by One- or Two-way ANOVAs or t-tests using GraphPad Prism software (La Jolla, CA). Significant main or interaction effects were followed by appropriate multiple comparisons tests. The criterion for significance was set at $p<0.05$. Data are shown as the mean ± SEM.

2.15. Code and Data availability

All next generation sequencing files associated with this study as well as the code that was used to pre-process and run differential expression are available online https://avm27.github.io/Methamphetamine_MicroglialRNASequencing_Analysis/.

3. Results

3.1. Mice acquire and maintain stable methamphetamine-taking, and demonstrate methamphetamine-seeking following forced home cage abstinence

To profile microglial gene expression changes during methamphetamine-taking and -seeking, we first established a method for METH IVSA. Mice underwent METH IVSA and forced home cage abstinence according to the timeline (**Fig. 1A**). Mice self-administered significantly more methamphetamine than saline during Maintenance (**Fig. 1B**) (Two-way RM ANOVA; METH vs Saline, $F(1, 19)=25.75$, $p<0.0001$). Additionally, mice self-administering methamphetamine displayed robust lever discrimination, while saline-

taking mice did not (**Fig. 1C**) (Two-way RM ANOVA; Active vs Inactive Lever, $F(3, 38)=29.49$, $p<0.0001$; METH vs Saline, $F(1, 19)=17.46$, $p=0.0005$). Following Abstinence, mice underwent a 2-hr context-induced reinstatement session (**Fig 1D**). Mice that previously self-administered methamphetamine showed increased active-lever responding (**Fig. 1E**) (Two-way RM ANOVA; METH Maint vs Reinst, $F(1, 19)=6.928$, $p=0.0164$; METH vs Saline Reinst, $F(1, 19)=11.73$, $p=0.0028$), as well as significant lever discrimination compared to control mice that had self-administered saline (**Fig. 1F**) (Two-way ANOVA; METH Active vs Inactive Lever, $F(1, 38)=13.82$, $p=0.0006$; METH vs Saline, $F(1, 38)=6.297$, $p=0.0165$). Indeed, in our model of METH IVSA, operant responding was higher for mice infusing methamphetamine than mice infusing saline, supporting the reinforcing properties of methamphetamine. Further, mice exhibited a high degree of lever discrimination when self-administering methamphetamine and showed higher rate of increase in active lever pressing during the reinstatement session, demonstrating the ability of this model to recapitulate methamphetamine-taking and -seeking behavior.

3.2. Methamphetamine self-administration induces persistent transcriptional changes on striatal microglia

Microglia tightly regulate their gene expression in response to their environment (Ayata, Badimon et al. 2018, Masuda, Sankowski et al. 2019, Yeh and Ikezu 2019). With a working model of METH IVSA, we next investigated how microglia in the striatum, a brain region known for its role in methamphetamine-related behaviors (Chang, Alicata et al. 2007, Li, Rubio et al. 2015), alter their transcriptome in response to METH (or saline) IVSA and following 21 days of forced home cage abstinence (**Fig. 2A**). RNA-sequencing of isolated striatal microglia revealed numerous significant differentially expressed genes (DEGs) in response to methamphetamine (**Fig. 2B-D**). Methamphetamine administration induced more significantly up- than downregulated genes in striatal microglia (342 increased vs 190 decreased; Maintenance vs Saline, adjusted p-value < 0.05 and L2FC > 1.3 (**Fig. 2B**). Additionally, prolonged abstinence resulted in a similar number of significantly up- and downregulated genes (316 increased vs 358 decreased; Abstinence vs Maintenance, adjusted p-value < 0.05 and L2FC > 1.3 or L2FC < -1.3 (**Fig. 2C**). Notably, many genes following 21 days of abstinence were significantly up- than downregulated (240 increased vs 69 decreased; Abstinence vs Saline, adjusted p-value < 0.05 and L2FC > 1.3 (**Fig. 2D**). Gene expression across highly differentially expressed genes show similarity amongst samples from the same groups (**Fig. 2E**). Importantly, hierarchical clustering of samples within each condition based on DE genes indicates that mice exposed to methamphetamine (Maintenance and Abstinence) cluster more closely than to saline (**Supplementary Fig. 1**). These findings suggest methamphetamine significantly alters the transcriptome of striatal microglia. Considering that microglial function is directly tied to their gene expression and adapts to the shifting neural environment, we sought to identify the biological nature of these transcriptional differences to better understand underlying molecular changes in response to methamphetamine.

To this end, Gene ontology (GO) pathway analysis of significant DE genes revealed enrichment of biological pathways related to protein folding, mRNA processing, and cytoskeleton organization due to methamphetamine-taking (Maintenance vs Saline) (**Fig. 3A**). Of note, methamphetamine administration

273 increased the expression of several heat shock proteins (e.g., Hspa8, Hspd1, Cryab, Ahsa2, and Dnaja1)
274 (**Fig. 3B**). When comparing microglia from methamphetamine-abstinent to methamphetamine-taking mice
275 (Abstinence vs Maintenance) pathways related to immune signaling and cellular stress response (e.g.,
276 apoptosis and response to radiation) were enriched (**Fig. 4A**). Specifically, compared to methamphetamine-
277 taking mice, striatal microglia from methamphetamine-abstinent mice showed decreased expression of
278 multiple heat shock proteins and apoptosis-related genes (e.g., Bax, Ddit3, Bclaf1, Acin1), yet increased
279 expression of oxidative stress-related genes (e.g., Cirbp, Fus, and Kcnb1), and dysregulated immune
280 signaling (e.g., Cd276, Nr1d1) (**Fig. 4B**). Finally, pathways related to synapse organization and nervous
281 system development were enriched in methamphetamine-abstinent mice (Abstinence vs Saline) (**Fig. 5A**).
282 Additionally, while heat shock proteins were generally downregulated when comparing Abstinence to
283 Maintenance, several were still upregulated when comparing Abstinence to Saline (e.g., Cryab, Hspa1a,
284 Dnaja1). Furthermore, striatal microglia from methamphetamine-abstinent mice exhibited dysregulation of
285 genes related to microglial activation (e.g., Syt11, Clu, Nr1d1) and upregulation of cell adhesion and
286 morphology-related genes (e.g., Adora1, Ddr1, Tppp) (**Fig. 5B**). Overall, these findings suggest striatal
287 microglia exhibit a unique transcriptome in response to methamphetamine administration and adopt a
288 neuroprotective phenotype promoting neurogenesis, cell survival, and resolution of neuroinflammation after
289 prolonged abstinence.
290

291 **3.3. Methamphetamine administration induces lasting changes in the morphology of striatal**
292 **microglia**

293 Microglial activity can be reflected in their morphology (Savage, Carrier et al. 2019, Vidal-Itriago,
294 Radford et al. 2022). Specifically, "surveilling" microglia assume a more ramified morphology, while "effector"
295 microglia deviate from this morphology (e.g., ameboid, hyper-ramified, etc.) (Morrison, Young et al. 2017,
296 Savage, Carrier et al. 2019). Secondary to the transcriptome analysis in the previous section, we sought to
297 determine if striatal microglia show persistent changes in their morphology during METH (or saline) IVSA and
298 following prolonged abstinence. Representative fluorescent images of striatal microglia are shown in **Fig.**
299 **6A**. We employed Sholl analysis, a method of quantifying branching complexity (Sholl 1953), to assess
300 morphological changes. Sholl analysis revealed microglia in methamphetamine-taking (Maintenance) and
301 methamphetamine-abstinent (Abstinence) mice were significantly less ramified than Saline-taking (Saline)
302 mice (**Fig. 6B**) (Two-way ANOVA; Distance x Condition Interaction, $F(44, 2875)=4.544$, $p<0.0001$).
303 Furthermore, methamphetamine administration reduced the number of intersections per cell (**Fig. 6C**) (One-
304 way ANOVA; Maintenance vs Saline, $p=0.0001$), as well as reduced the length and number (**Fig. 6D**) **(**One-
305 way ANOVA; Maintenance vs Saline, $p=0.0002$) of branches (**Fig. 6E**) (One-way ANOVA; Maintenance vs
306 Saline, $p=0.00027$) of striatal microglia. Of note, this effect persists 21 days into abstinence (One-way
307 ANOVA; Abstinence vs Saline Total Intersections, $p<0.0001$; Abstinence vs Saline Mean Intersections,
308 $p<0.0001$; Abstinence vs Saline Max Branch Length, $p<0.0038$). Taken as a whole, these data demonstrate
309 that striatal microglia adopt an altered morphology in response to methamphetamine, and that these changes
310 last for several weeks following final methamphetamine exposure. Furthermore, given the neurotoxicity of

methamphetamine (Asanuma, Miyazaki et al. 2004, Jayanthi, Daiwile et al. 2021) these results are consistent with previous findings illustrating microglial reactivity following methamphetamine administration (Thomas, Walker et al. 2004, Robson, Turner et al. 2013, Goncalves, Leitao et al. 2017) and abstinence (Sekine, Ouchi et al. 2008, Yu, Chen et al. 2023).

3.4. Microglial depletion during active methamphetamine-taking increases drug-intake.

Methamphetamine administration induced persistent transcriptional and morphological changes in striatal microglia, suggesting a possible role in drug-taking behavior. To this end, we ablated microglia with PLX5622 during methamphetamine-taking (Acquisition and Maintenance). We found that mice self-administered methamphetamine regardless of treatment (**Fig. 7B**) (Two-way RM ANOVA; AIN-76A vs PLX5622, $F(1, 17)=1.885$, $p=0.1876$). Yet, while mice treated with AIN-76A showed stable intake across Maintenance, mice treated with PLX5622 gradually increased their methamphetamine intake (**Fig. 7C**) (t-test with Welch's correction; AIN-76A vs PLX5622, $p=0.0360$). Additionally, while both treatment groups demonstrated robust discrimination between active and inactive levers over time (**Fig. 7D**) (Two-way RM ANOVA; Interaction between Session and Lever, $F(42, 476)=1.832$, $p=0.0016$), mice lacking microglia pressed the active lever significantly more than control mice by the end of Maintenance (**Fig. 7E**) (Two-way ANOVA; Active vs Inactive Lever, $F(1, 34)=48.41$, $p<0.0001$; AIN-76A vs PLX5622, $F(1, 34)=4.113$, $p=0.0505$). These data show that microglial ablation increases methamphetamine self-administration, and as such, suggests that microglia may regulate the reinforcing properties of methamphetamine.

3.5. Microglial depletion during forced home cage abstinence does not affect context-induced methamphetamine-seeking.

Since we found microglia to contribute to methamphetamine-taking behavior, we sought to determine if microglia contribute to methamphetamine-seeking. To this end, mice underwent METH IVSA, then were assigned to treatment groups (AIN-76A or PLX5622) for the duration of 21-day home cage abstinence (**Fig. 8A**). Importantly, treatment groups did not differ in number of methamphetamine infusions earned (**Fig. 8B**) (t-test with Welch's correction; AIN-76A vs PLX5622, $p= 0.5724$) or lever discrimination (**Fig. 8C**) (Two-way ANOVA; Active vs Inactive Lever, $F(1, 32)=109.3$, $p<0.0001$; AIN-76A vs PLX5622, $F(1, 32)=0.3010$, $p=0.5870$) prior to abstinence (combined data shown). We found that microglial depletion failed to significantly attenuate context-induced reinstatement following forced home cage abstinence (**Fig. 8D**) (Two-way ANOVA; Maint vs Reinst, $F(1, 16)=16.29$, $p=0.0010$; AIN-76A vs PLX5622, $F(1, 16)=0.06173$, $p=0.8069$). Additionally, both treatment groups displayed significant lever discrimination during the reinstatement session (**Fig. 8E**) (Two-way ANOVA; Active vs Inactive Lever, $F(1, 32)=46.16$, $p<0.0001$; AIN-76A vs PLX5622, $F(1, 32)=0.03116$, $p=0.8610$), suggesting a learned association between active lever pressing and reinforcement-seeking. Thus, these results suggest that while microglia may regulate the reinforcing properties of methamphetamine-taking (**Fig. 7B, C**), these cells are not necessary for reinstatement of methamphetamine-seeking following prolonged abstinence.

4. Discussion

4.1. Striatal microglia adopt a unique transcriptome and alter their morphology in response to methamphetamine administration and following prolonged abstinence

Consistent with the literature, we find that methamphetamine administration results in upregulation of gene expression related to oxidative stress (Kuhn, Francescutti-Verbeem et al. 2006, Limanaqi, Gambardella et al. 2018, Yang, Wang et al. 2018). Specifically, methamphetamine administration resulted in a robust increase in heat shock protein expression, which has been linked to methamphetamine-induced hyperthermia (Cruickshank and Dyer 2009, Kiyatkin and Sharma 2011, Liao, Lu et al. 2021) and the production of reactive oxygen species from methamphetamine-induced neurotoxicity and terminal degeneration in the striatum (Asanuma, Miyazaki et al. 2004, McConnell, O'Banion et al. 2015, Frank, Adhikary et al. 2016). Importantly, many of these genes remained dysregulated following 21 days of abstinence, which is in agreement with human PET studies, where microglial activation persists 2 years after methamphetamine cessation (Sekine, Ouchi et al. 2008). Consistent with upregulation of genes related to cell adhesion (e.g., Tppp, Adora1, Tubb4a), morphological analysis revealed that striatal microglia have reduced branching complexity that remains through abstinence. Additionally, we found that following methamphetamine administration, striatal microglia share similar gene expression to disease-associated microglia from neurodegenerative diseases such as Alzheimer's (Corneveaux, Myers et al. 2010) and Parkinson's disease (PD) (Du, Wang et al. 2017). Notably, the upregulation of several genes associated with PD (e.g., Cryab, Syt11, Hspa8, Stip1) in our dataset support studies which have shown that individuals with methamphetamine use disorder are three times more likely to develop PD (Callaghan, Cunningham et al. 2012, Curtin, Fleckenstein et al. 2015), and suggest microglia may contribute to this increased risk. These results further suggest methamphetamine administration induces lasting effects on the neuronal environment and that microglia adapt to these environmental changes by altering their transcriptome, which is reflected in their morphology. Indeed, our data demonstrate microglia may adopt a more neuroprotective state during abstinence by modulating their gene expression in favor of nervous system development and repair (e.g., Ptgds, Nrxn1, Cntn1, Lgals1) (Colton 2009, Starossom, Mascanfroni et al. 2012, Hickman, Kingery et al. 2013), as well as promoting their own survival and proliferation (e.g., Dnaja1, Bnip3, Acin1, Hspa1a, Clu), thus indicating that microglia may assist in the resolution of inflammation and restoration of homeostasis in the striatal neural environment.

Considering the persistence of these transcriptional and morphological changes, the data suggest epigenetic mechanisms may also be involved. Although we did not find many significant epigenetic-related gene expression changes within our dataset, several studies have highlighted the importance of epigenetic regulation of gene expression following methamphetamine administration (Omonijo, Wongprayoon et al. 2014, Cadet, Brannock et al. 2015) and microglial activity (Matcovitch-Natan, Winter et al. 2016, Ayata, Badimon et al. 2018, Cheray and Joseph 2018). Specifically, H3K4 methylation and H3K27 acetylation, markers of active gene promoters and enhancers (Calo and Wysocka 2013), are linked to innate immune memory in macrophages (Kaikkonen, Spann et al. 2013, Ostuni, Piccolo et al. 2013) and more recently in microglia (Meleady, Towriss et al. 2023). These histone modifications, along with numerous other epigenetic

enzymes and chromatin remodeling complexes, have implicated microglia in the progression of neurodegenerative disease and aging (Cho, Chen et al. 2015, Yeh and Ikezu 2019, Huang, Malovic et al. 2023), as well as substance use disorders (Schwarz, Hutchinson et al. 2011, Crews, Coleman et al. 2023, Vilca, Margetts et al. 2023). Therefore, future studies are needed to examine the underlying epigenetic machinery in microglia that may govern the lasting transcriptional and morphological changes due to methamphetamine administration and following abstinence.

4.2. Are microglia protective against excessive methamphetamine-taking?

We found that methamphetamine administration is influenced by the absence of microglia, as microglial depletion during active methamphetamine-taking increases drug-intake. Importantly, microglial depletion does not affect operant conditioning (**Supplementary Fig. 2**), suggesting microglia specifically regulate the reinforcing properties of methamphetamine in our behavioral model. Interestingly, we found several genes involved in neurotransmitter signaling and synthesis to be upregulated in response to methamphetamine administration and following abstinence (**Supplementary Figs. 3 and 4**), underscoring the neurotransmitter-sensing capabilities of microglia and their ability to modulate neuronal activity and neurotransmitter release (Badimon, Strasburger et al. 2020, Stolero and Frenkel 2021). For example, microglia are thought to contribute to the reuptake of GABA (Bhandage and Barragan 2021, Favuzzi, Huang et al. 2021), a neurotransmitter that is elevated in the striatum during administration of and withdrawal from psychostimulants (Wydra, Golembiowska et al. 2013). Indeed, we found the GABA transporter 1 (GAT1) to be significantly upregulated during methamphetamine-taking and abstinence (**Supplementary Fig. 4**). Furthermore, several genes related to glutamate synaptic clearance (GLT-1), signaling (mGluR3, Gria2, Glrb), and processing (Glul, Glud1, Got1, Gls) were also increased following methamphetamine administration and abstinence (**Supplementary Fig. 4**) (van Landeghem, Stover et al. 2001). As such, eliminating microglia may disrupt homeostatic responses to methamphetamine aimed at maintaining excitatory/inhibitory balance in the striatum. Additionally, methamphetamine-induced upregulation of dopamine signaling genes (Gpr37, Ddc, Darpp-32, Cdh11) in striatal microglia (**Supplementary Fig. 3**) further suggests that these cells may alter their gene expression to adapt to increased striatal dopamine normally seen following methamphetamine administration (Mark, Soghomonian et al. 2004). Therefore, depleting microglia may impair endogenous mechanisms to maintain neurotransmitter balance in the striatum – an effect that becomes evident as animals gradually escalate intake over repeated methamphetamine self-administration sessions (**Fig. 7B**). Indeed, while the overall effect of microglial depletion could result in increased motivation for the drug, further studies will be necessary to explore these possible mechanisms.

Interestingly, while microglial depletion increased methamphetamine-taking, it was not sufficient to attenuate context-induced reinstatement of methamphetamine-seeking, suggesting microglia may not play a determining role in methamphetamine-seeking following abstinence. This finding is consistent with literature demonstrating that chronic delivery of the TLR4 antagonist (+)-naltrexone does not affect cue-induced reinstatement of methamphetamine-seeking after 13 days of abstinence (Theberge, Li et al. 2013). Additionally, a separate study showed global knockout of TNF-α increased methamphetamine self-

administration and motivation but did not affect cue-induced reinstatement (Yan, Nitta et al. 2012). However, in contrast, minocycline has been shown to mitigate methamphetamine-primed reinstatement (Attarzadeh-Yazdi, Arezoomandan et al. 2014), although the pharmacological profile of minocycline may engage relevant targets independent from microglia. Taken together, these data suggest methamphetamine-seeking may involve more complex mechanisms that are not microglial-dependent.

4.3. Limitations of the current study

Sex is an important consideration when studying MUD (McHugh, Votaw et al. 2018). Women have been reported to use methamphetamine earlier in life and become more dependent (Dluzen and Liu 2008). Additionally, neuroimmune system development is regulated by sex (McCarthy, Nugent et al. 2017, Osborne, Turano et al. 2018). Consequently, a limitation of the current study was only using male mice for the behavioral and molecular experiments. Also of note, while the current study examined striatal microglia, as this brain region has been heavily implicated in the development and maintenance of MUD (Chang, Alicata et al. 2007), other brain regions such as the hippocampus (Goncalves, Baptista et al. 2010, Takashima, Fannon et al. 2018) and various cortical regions (Gonzalez, Jayanthi et al. 2018, Kearns, Siemsen et al. 2022) also contribute to methamphetamine-related behaviors and pathophysiology of MUD, as well as transcriptional differences in microglia (Barko, Shelton et al. 2022). Therefore, further studies focusing on sex differences and relevant brain regions beyond the striatum will be necessary to gain a better understanding of the underlying microglial mechanisms regulating methamphetamine reinforcement.

5. Conclusion

In conclusion, our data suggest that microglia adopt a persistent neuroprotective phenotype in response to methamphetamine administration. In addition, methamphetamine-induced dysregulation of GABA and glutamate neurotransmission genes suggest that microglia may also play a role in methamphetamine reinforcement beyond neuroimmune regulation, an effect supported by increased methamphetamine-taking in the absence of microglia. Altogether, this study increases our understanding of how microglia adapt their gene expression and morphology to methamphetamine administration and seeking and may provide insights into the role of microglia in the methamphetamine reinforcement and methamphetamine use disorder pathophysiology.

Acknowledgments

SJV, AVM, and LMT designed and coordinated the study. SJV conducted all behavioral experiments and obtained samples for RNA sequencing and IHC. SJV and AVM processed samples for RNA sequencing, and SJV and IF processed samples for IHC. SJV and AVM conducted statistical analysis and data interpretation. SJV, AVM, and LMT drafted the manuscript. IF was supported by NCI grant R25CA261632. This work was supported by NIDA grants K01DA045294 (LMT), DP1DA051828 (LMT), U18DA052533 (CW), NINDS grant F99NS130871 (SJV), the NIDA Drug Supply Program, as well as a kind gift from the Shipley Foundation (LMT).

Figure 1

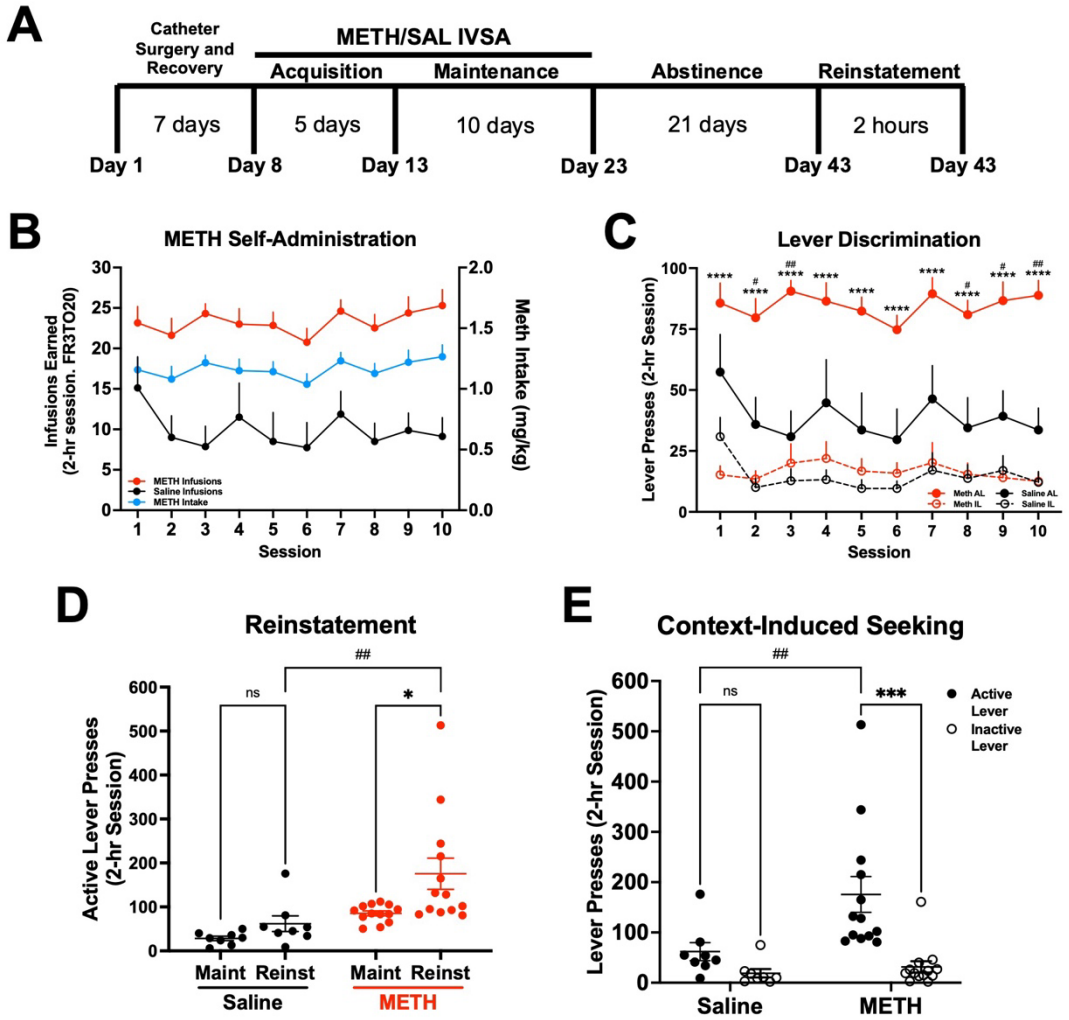

Figure 1. Establishment of a mouse model of METH IV self-administration. Male C57BL/6J mice were trained to self-administer METH (n=13) or Saline (n=8) during daily 2-hr sessions at FR3TO20. **A)** Experimental timeline. **B)** METH and Saline infusions earned, and METH consumed, during 15 daily 2-hr sessions (FR3TO20). **C)** Active lever presses for Maintenance (**Maint**: average final 3 days) and Reinstatement (**Reinst**) of METH or Saline-seeking. Two-way RM ANOVA with Bonferroni post-hoc test (METH Maint vs Reinst *$p<0.05$; METH vs Saline Reinst $^{##}p<0.01$). **D)** Active and inactive lever presses during Reinstatement. Two-way ANOVA with Bonferroni's post-hoc test (METH Active vs Inactive Lever, ***$p<0.001$; METH Active vs Saline Active, $^{##}p<0.01$). Data are represented as mean ± SEM.

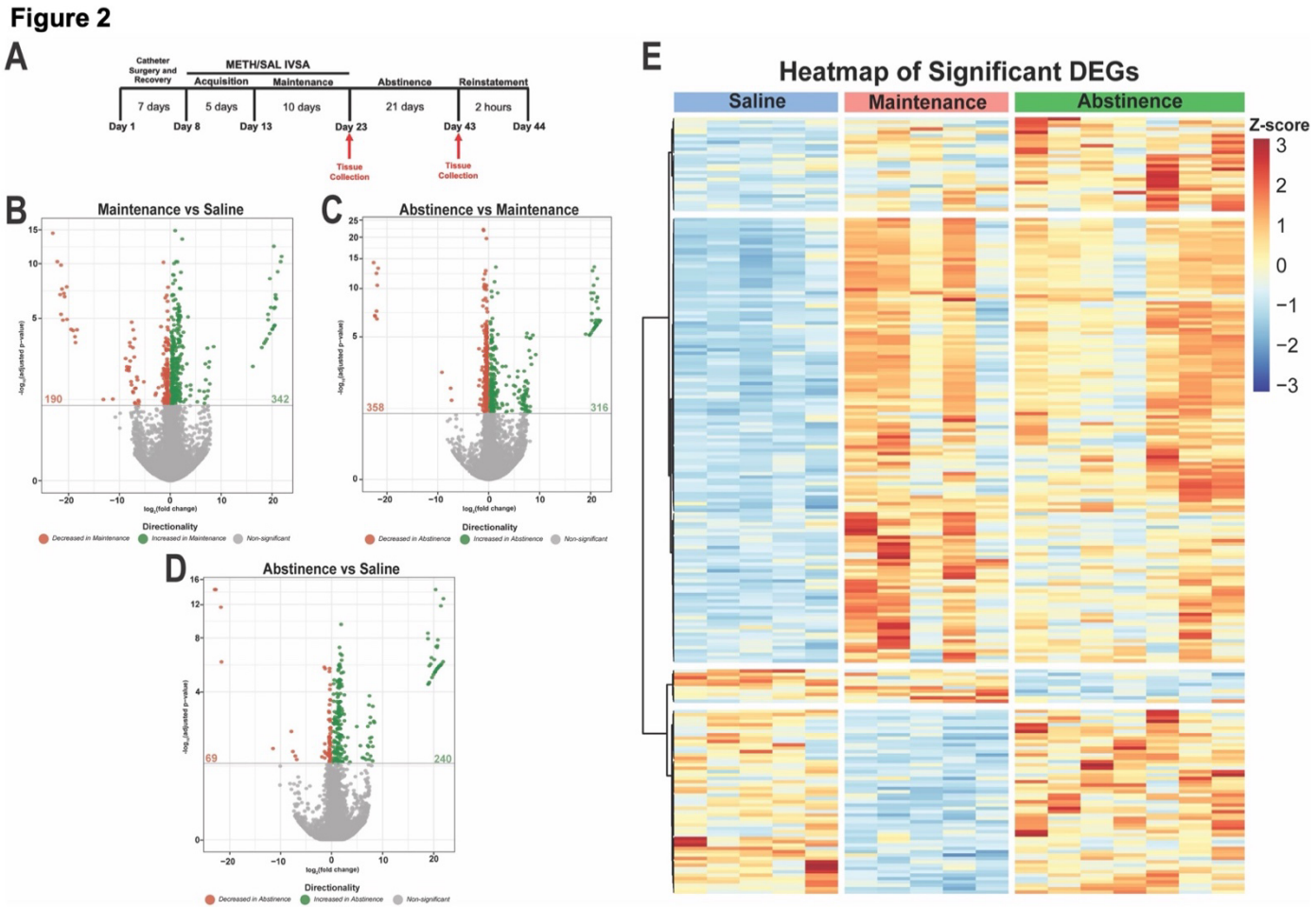

Figure 2. METH self-administration induces distinct transcriptional profiles in striatal microglia. A) Experimental timeline. Volcano plots showing significant DE genes (Log2FC vs -$\log_{10}$ adjusted p-value) in **B)** Maintenance vs Saline, **C)** Abstinence vs Maintenance, and **D)** Abstinence vs Saline. Red (decreased) and green (increased) circles represent DE genes that reached significance based on adjusted p-value < 0.05. **E)** Heatmap of normalized counts (rlog transformed) of selected significant DE genes (adjusted p-value < 0.05, lfcSE ≤ 1.5, L2FC ≤ -1.3 and L2FC ≥ 1.3) for each condition clustered by gene. Each column represents a single animal (Saline, blue; Maintenance, red; Abstinence, green).

Figure 3

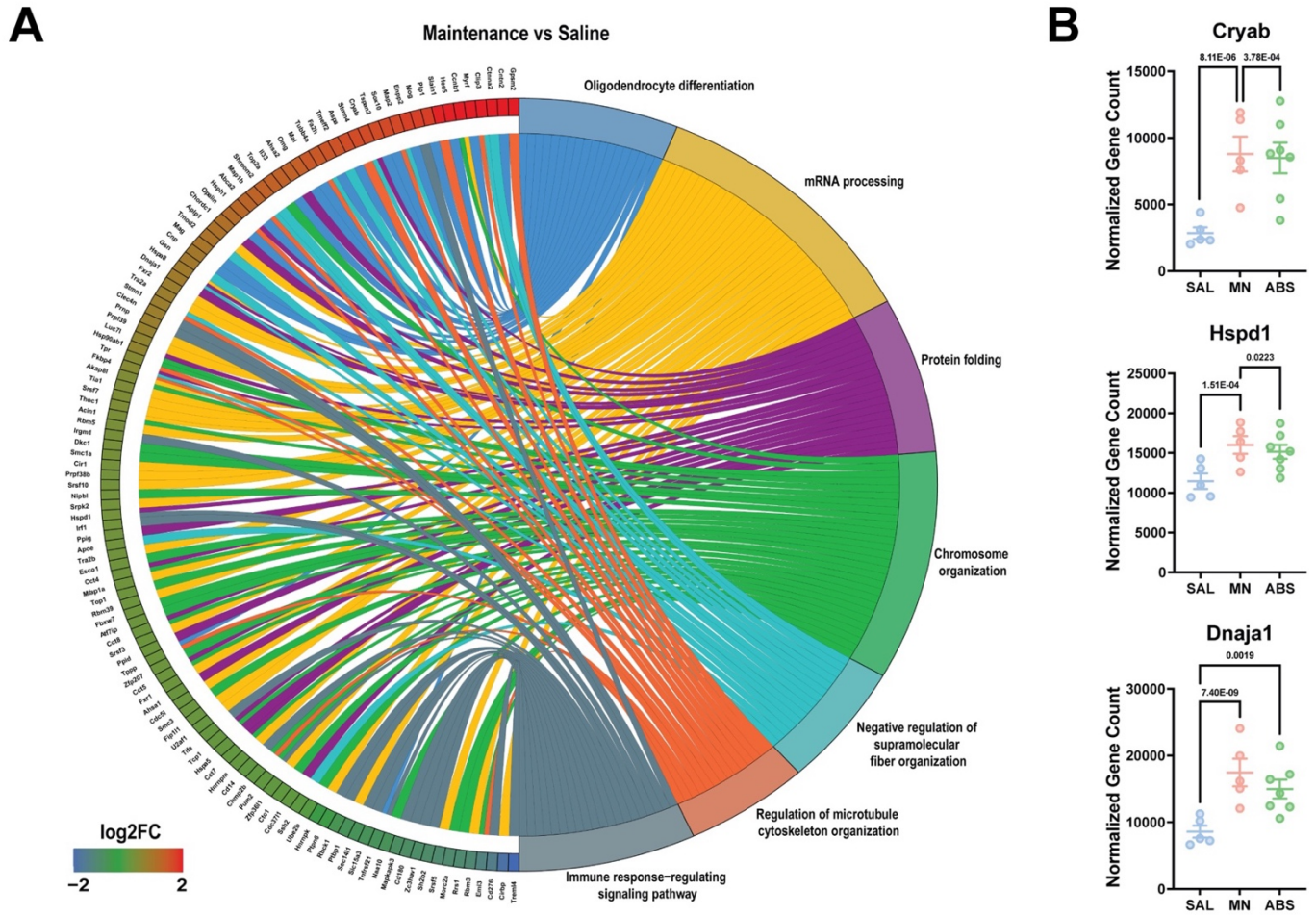

Figure 3. Gene Ontology (GO) enrichment analysis reveals dysregulation of protein folding and mRNA processing following METH self-administration. A) Chord plot showing interaction between GO biological process terms and genes comparing Maintenance vs Saline. **B)** Normalized counts of significant DE genes with adjusted p-value for each comparison.

Figure 4

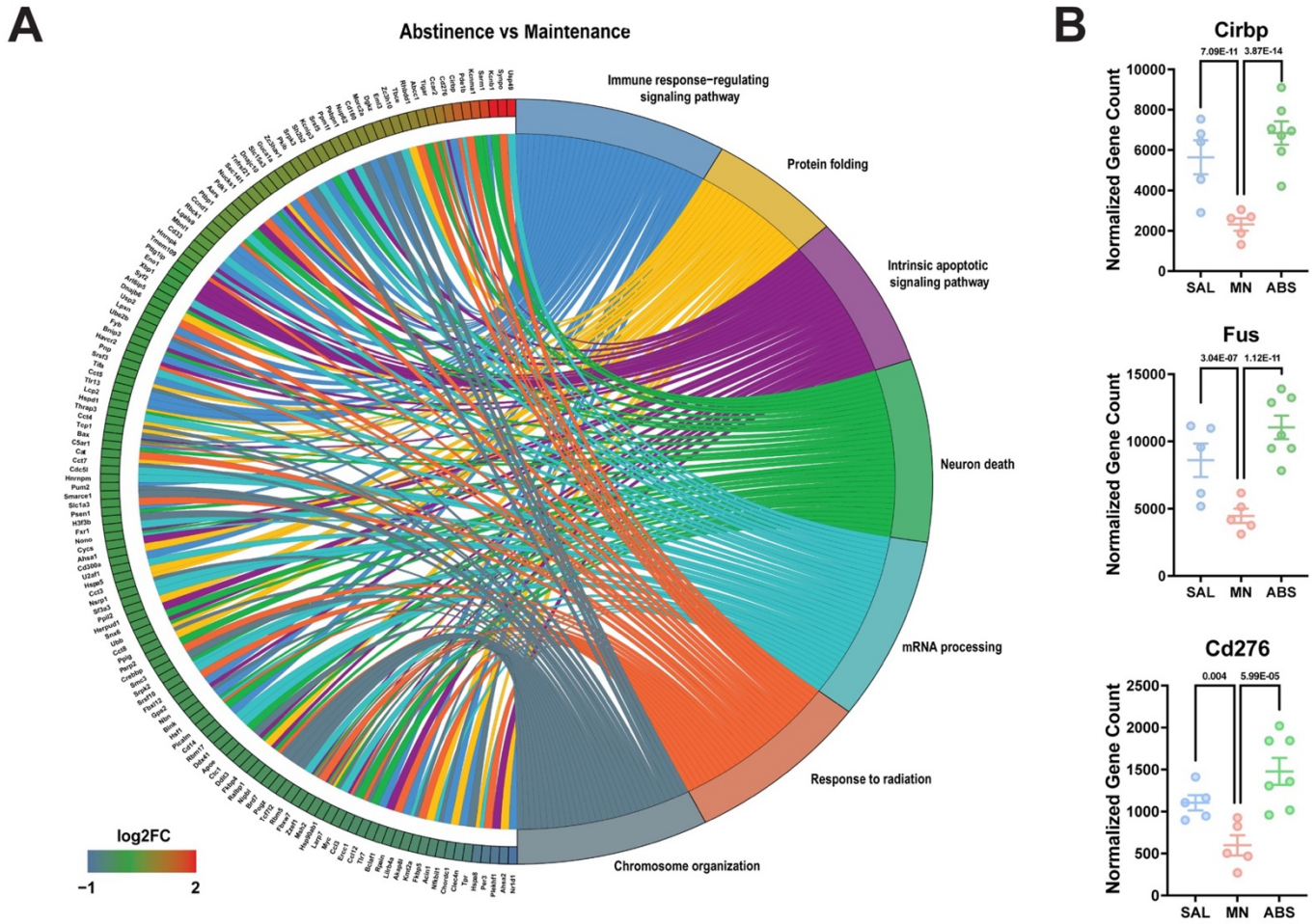

Figure 4. Gene Ontology (GO) enrichment analysis reveals dysregulation of immune signaling and cellular stress response in microglia previously exposed to METH. A) Chord plot showing interaction between GO biological process terms and genes comparing Abstinence vs Maintenance, **B)** Normalized counts of significant DE genes with adjusted p-value for each comparison.

Figure 5

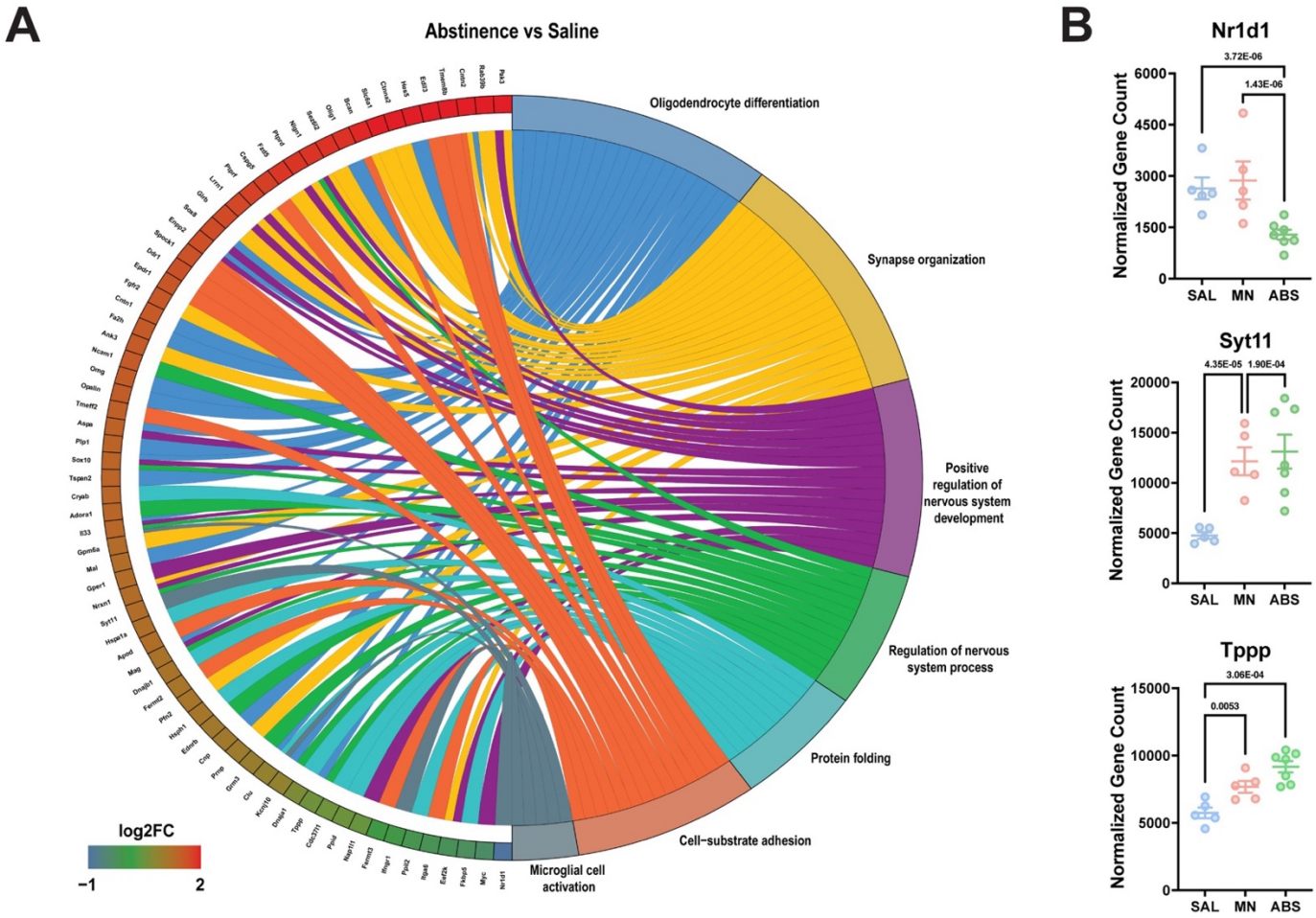

494

495 **Figure 5. Gene Ontology (GO) enrichment analysis reveals persistent dysregulation of cell adhesion**
496 **and microglial activation during abstinence. A)** Chord plot showing interaction between GO biological
497 process terms and genes comparing Abstinence vs Saline, **B)** Normalized counts of significant DE genes
498 with adjusted p-value for each comparison.

Figure 6

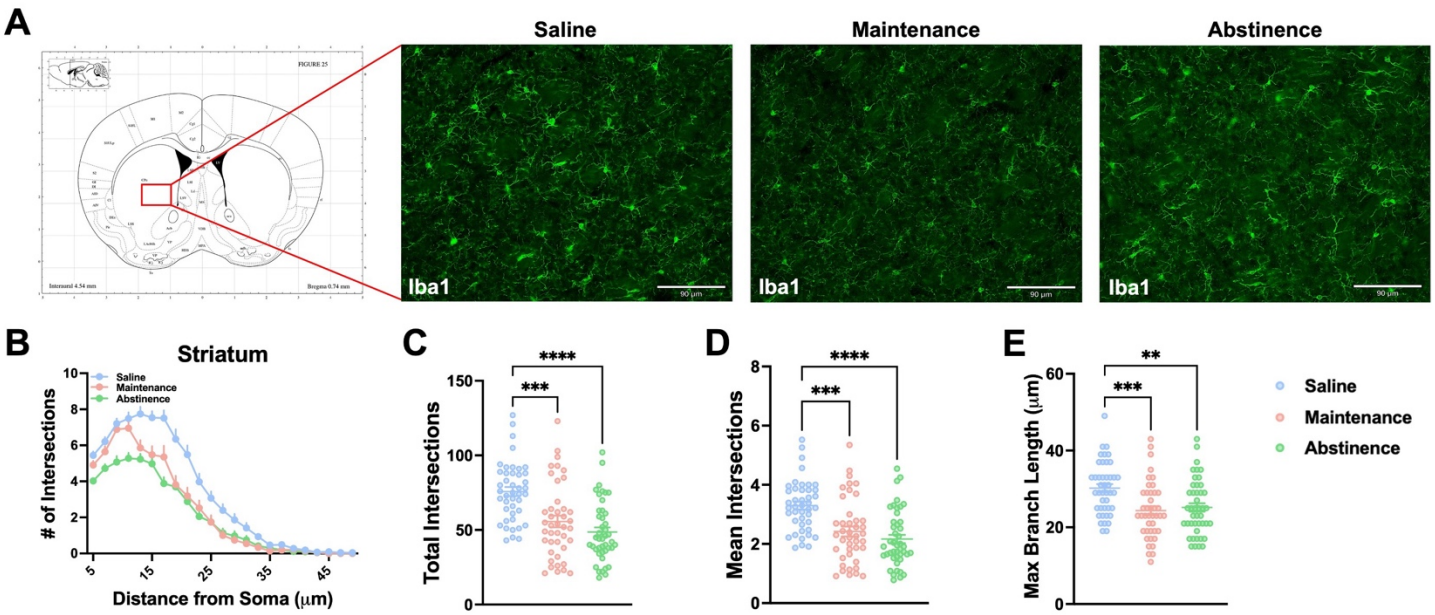

Figure 6. Striatal microglia exhibit persistent altered morphology following METH self-administration. A) Representative fluorescent images (Bregma 0.7-0.8 mm, Paxinos and Franklin's the Mouse Brain in Stereotaxic Coordinates) of microglia (Iba1^{+} cells) in the striatum. **B)** Sholl analysis plot of microglia. **C-E)** Mice that self-administered METH (Maintenance), as well as METH-abstinent mice (Abstinence), display less ramifications and branching and shorter processes than Saline-taking mice (Saline). One-way ANOVA with Tukey post-hoc test (Between Conditions, **p<0.01, ***p<0.001, ****p<0.0001). 40-43 cells (10-12 cells from n=4 mice) per condition. Data are represented as mean ± SEM. Scale bar 90 μm.

Figure 7

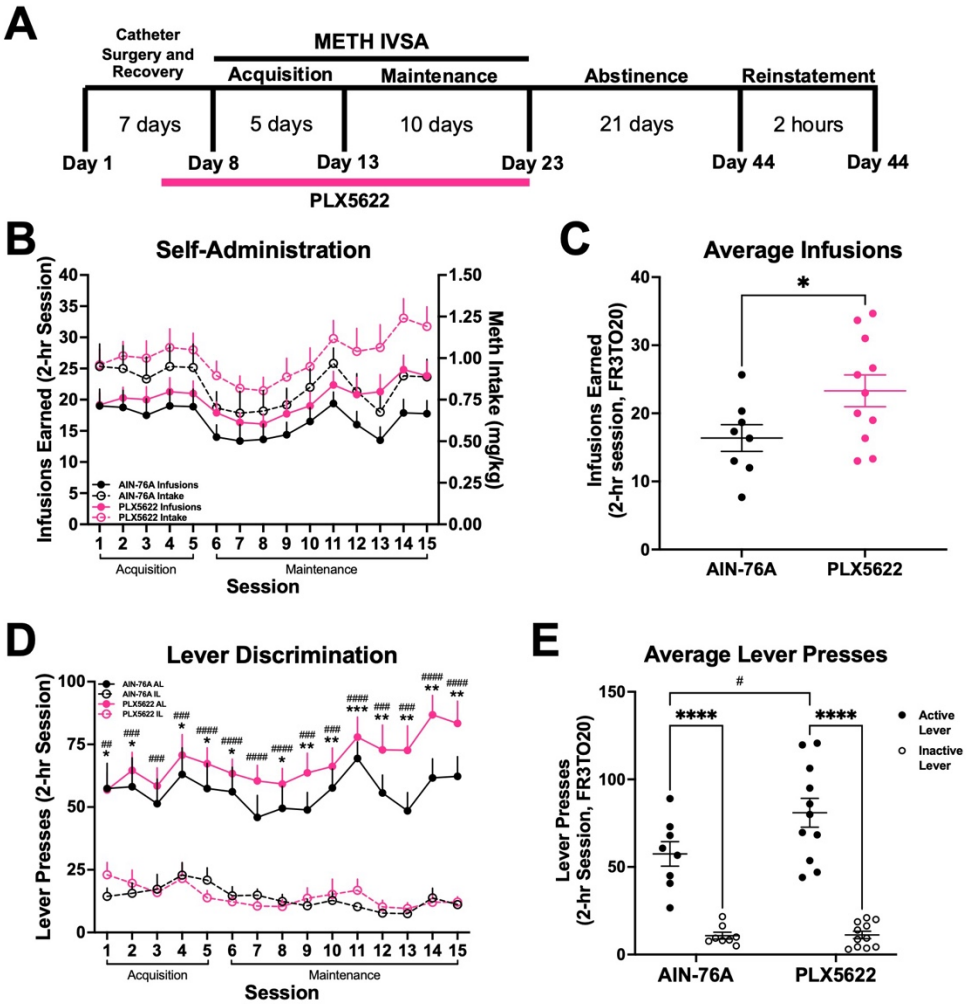

Figure 7. Microglial depletion increases METH self-administration. A) Experimental timeline. **B)** METH intake and infusions earned during 15 daily 2-hr sessions (FR3TO20). **C)** Average infusions earned over the last 3 days of Maintenance. Unpaired t-test with Welch's correction (AIN-76A vs PLX5622, *p<0.05). **D)** Active and inactive lever presses during 15 daily 2-hour sessions (FR3TO20). Two-way RM ANOVA with Bonferroni's post-hoc test, (AIN-76A Active vs Inactive Lever, *p<0.05, **p<0.01, ***p<0.001; PLX5622 Active vs Inactive Lever, $^{\#}$p<0.05, $^{\#\#}$p<0.01, $^{\#\#\#}$p<0.001, $^{\#\#\#\#}$p<0.0001) **E)** Average active and inactive lever presses over the last 3 days of Maintenance. Two-way ANOVA with Bonferroni's post-hoc test (Active vs Inactive Lever, ****p<0001; AIN-76A Active vs PLX5622 Active, $^{\#}$p<0.05). AIN-76A (n=8), PLX5622 (n=11). Data are represented as mean ± SEM.

Figure 8

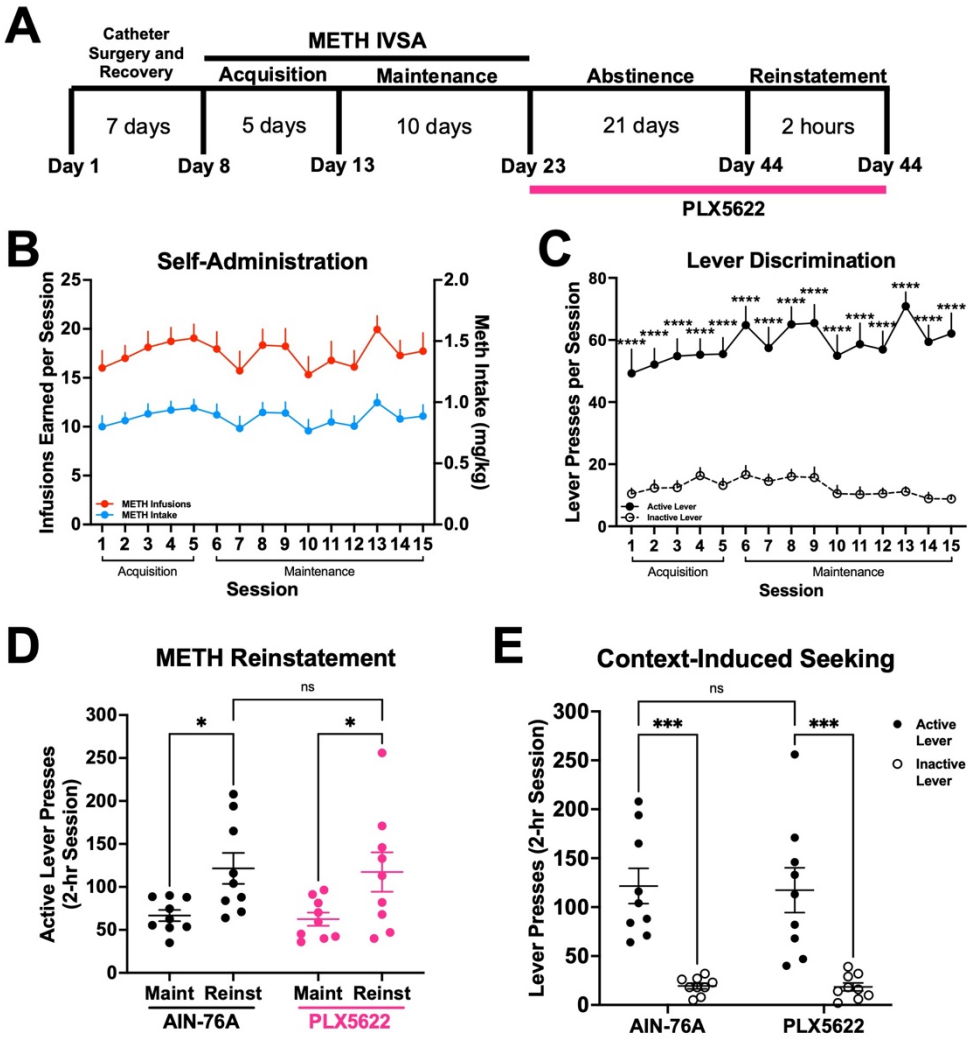

Figure 8. Microglial depletion does not affect context-induced drug-seeking. A) Experimental timeline. **B)** METH intake and infusions earned during 15 daily 2-hr sessions. **C)** Active and inactive lever presses. Two-way RM ANOVA with Bonferroni's post-hoc test, (Active vs Inactive Lever, ****p<0.0001). **D)** Active lever presses for Maintenance (**Maint**: average final 3 days) and Reinstatement (**Reinst**) of AIN-76A and PLX5622. Two-way RM ANOVA with Bonferroni post-hoc test (AIN-76A Maint vs Reinst, *p<0.05; PLX5622 Maint vs Reinst, *p<0.05; AIN-76A vs PLX5622 Reinst, ns=non-significant). **E)** Active and inactive lever presses during Reinstatement. Two-way ANOVA with Bonferroni's post-hoc test (Active vs Inactive Lever, ***p<0.001, AIN-76A vs PLX5622 Active Lever, ns=non-significant). AIN-76A (n=9), PLX5622 (n=9). Data are represented as mean ± SEM.

527 **References**

528 Asanuma, M., I. Miyazaki, Y. Higashi, T. Tsuji and N. Ogawa (2004). "Specific gene expression and possible
529 involvement of inflammation in methamphetamine-induced neurotoxicity." Ann N Y Acad Sci **1025**: 69-75.

530 Attarzadeh-Yazdi, G., R. Arezoomandan and A. Haghparast (2014). "Minocycline, an antibiotic with inhibitory
531 effect on microglial activation, attenuates the maintenance and reinstatement of methamphetamine-seeking
532 behavior in rat." Prog Neuropsychopharmacol Biol Psychiatry **53**: 142-148.

533 Ayata, P., A. Badimon, H. J. Strasburger, M. K. Duff, S. E. Montgomery, Y. E. Loh, A. Ebert, A. A. Pimenova,
534 B. R. Ramirez, A. T. Chan, J. M. Sullivan, I. Purushothaman, J. R. Scarpa, A. M. Goate, M. Busslinger, L.
535 Shen, B. Losic and A. Schaefer (2018). "Epigenetic regulation of brain region-specific microglia clearance
536 activity." Nat Neurosci **21**(8): 1049-1060.

537 Badimon, A., H. J. Strasburger, P. Ayata, X. Chen, A. Nair, A. Ikegami, P. Hwang, A. T. Chan, S. M. Graves,
538 J. O. Uweru, C. Ledderose, M. G. Kutlu, M. A. Wheeler, A. Kahan, M. Ishikawa, Y. C. Wang, Y. E. Loh, J. X.
539 Jiang, D. J. Surmeier, S. C. Robson, W. G. Junger, R. Sebra, E. S. Calipari, P. J. Kenny, U. B. Eyo, M.
540 Colonna, F. J. Quintana, H. Wake, V. Gradinaru and A. Schaefer (2020). "Negative feedback control of
541 neuronal activity by microglia." Nature **586**(7829): 417-423.

542 Barko, K., M. Shelton, X. Xue, Y. Afriyie-Agyemang, S. Puig, Z. Freyberg, G. C. Tseng, R. W. Logan and M.
543 L. Seney (2022). "Brain region- and sex-specific transcriptional profiles of microglia." Front Psychiatry **13**:
544 945548.

545 Barr, A. M., W. J. Panenka, G. W. MacEwan, A. E. Thornton, D. J. Lang, W. G. Honer and T. Lecomte (2006).
546 "The need for speed: an update on methamphetamine addiction." J Psychiatry Neurosci **31**(5): 301-313.

547 Bhandage, A. K. and A. Barragan (2021). "GABAergic signaling by cells of the immune system: more the rule
548 than the exception." Cell Mol Life Sci **78**(15): 5667-5679.

549 Cadet, J. L., C. Brannock, S. Jayanthi and I. N. Krasnova (2015). "Transcriptional and epigenetic substrates
550 of methamphetamine addiction and withdrawal: evidence from a long-access self-administration model in the
551 rat." Mol Neurobiol **51**(2): 696-717.

552 Callaghan, R. C., J. K. Cunningham, J. Sykes and S. J. Kish (2012). "Increased risk of Parkinson's disease
553 in individuals hospitalized with conditions related to the use of methamphetamine or other amphetamine-type
554 drugs." Drug Alcohol Depend **120**(1-3): 35-40.

555 Calo, E. and J. Wysocka (2013). "Modification of enhancer chromatin: what, how, and why?" Mol Cell **49**(5):
556 825-837.
557 Canedo, T., C. C. Portugal, R. Socodato, T. O. Almeida, A. F. Terceiro, J. Bravo, A. I. Silva, J. D. Magalhaes,
558 S. Guerra-Gomes, J. F. Oliveira, N. Sousa, A. Magalhaes, J. B. Relvas and T. Summavielle (2021).
559 "Astrocyte-derived TNF and glutamate critically modulate microglia activation by methamphetamine."
560 Neuropsychopharmacology **46**(13): 2358-2370.
561 CDC, N. (2021). "CDC WONDER Online Database “Multiple Cause of Death, 1999-2020”."
562 Chang, L., D. Alicata, T. Ernst and N. Volkow (2007). "Structural and metabolic brain changes in the striatum
563 associated with methamphetamine abuse." Addiction **102 Suppl 1**: 16-32.
564 Chao, J., Y. Zhang, L. Du, R. Zhou, X. Wu, K. Shen and H. Yao (2017). "Molecular mechanisms underlying
565 the involvement of the sigma-1 receptor in methamphetamine-mediated microglial polarization." Sci Rep **7**(1):
566 11540.
567 Cheray, M. and B. Joseph (2018). "Epigenetics Control Microglia Plasticity." Front Cell Neurosci **12**: 243.
568 Cho, S. H., J. A. Chen, F. Sayed, M. E. Ward, F. Gao, T. A. Nguyen, G. Krabbe, P. D. Sohn, I. Lo, S. Minami,
569 N. Devidze, Y. Zhou, G. Coppola and L. Gan (2015). "SIRT1 deficiency in microglia contributes to cognitive
570 decline in aging and neurodegeneration via epigenetic regulation of IL-1beta." J Neurosci **35**(2): 807-818.
571 Colton, C. A. (2009). "Heterogeneity of microglial activation in the innate immune response in the brain." J
572 Neuroimmune Pharmacol **4**(4): 399-418.
573 Corneveaux, J. J., A. J. Myers, A. N. Allen, J. J. Pruzin, M. Ramirez, A. Engel, M. A. Nalls, K. Chen, W. Lee,
574 K. Chewning, S. E. Villa, H. B. Meechoovet, J. D. Gerber, D. Frost, H. L. Benson, S. O'Reilly, L. B. Chibnik,
575 J. M. Shulman, A. B. Singleton, D. W. Craig, K. R. Van Keuren-Jensen, T. Dunckley, D. A. Bennett, P. L. De
576 Jager, C. Heward, J. Hardy, E. M. Reiman and M. J. Huentelman (2010). "Association of CR1, CLU and
577 PICALM with Alzheimer's disease in a cohort of clinically characterized and neuropathologically verified
578 individuals." Hum Mol Genet **19**(16): 3295-3301.
579 Crews, F. T., L. G. Coleman, Jr., V. A. Macht and R. P. Vetreno (2023). "Targeting Persistent Changes in
580 Neuroimmune and Epigenetic Signaling in Adolescent Drinking to Treat Alcohol Use Disorder in Adulthood."
581 Pharmacol Rev **75**(2): 380-396.

582 Cruickshank, C. C. and K. R. Dyer (2009). "A review of the clinical pharmacology of methamphetamine."
583 Addiction **104**(7): 1085-1099.
584 Curtin, K., A. E. Fleckenstein, R. J. Robison, M. J. Crookston, K. R. Smith and G. R. Hanson (2015).
585 "Methamphetamine/amphetamine abuse and risk of Parkinson's disease in Utah: a population-based
586 assessment." Drug Alcohol Depend **146**: 30-38.
587 Dluzen, D. E. and B. Liu (2008). "Gender differences in methamphetamine use and responses: a review."
588 Gend Med **5**(1): 24-35.
589 Du, C., Y. Wang, F. Zhang, S. Yan, Y. Guan, X. Gong, T. Zhang, X. Cui, X. Wang and C. X. Zhang (2017).
590 "Synaptotagmin-11 inhibits cytokine secretion and phagocytosis in microglia." Glia **65**(10): 1656-1667.
591 Everitt, B. J. and T. W. Robbins (2005). "Neural systems of reinforcement for drug addiction: from actions to
592 habits to compulsion." Nat Neurosci **8**(11): 1481-1489.
593 Favuzzi, E., S. Huang, G. A. Saldi, L. Binan, L. A. Ibrahim, M. Fernandez-Otero, Y. Cao, A. Zeine, A. Sefah,
594 K. Zheng, Q. Xu, E. Khlestova, S. L. Farhi, R. Bonneau, S. R. Datta, B. Stevens and G. Fishell (2021).
595 "GABA-receptive microglia selectively sculpt developing inhibitory circuits." Cell **184**(15): 4048-4063 e4032.
596 Ferreira, T. A., A. V. Blackman, J. Oyrer, S. Jayabal, A. J. Chung, A. J. Watt, P. J. Sjostrom and D. J. van
597 Meyel (2014). "Neuronal morphometry directly from bitmap images." Nat Methods **11**(10): 982-984.
598 Frank, M. G., S. Adhikary, J. L. Sobesky, M. D. Weber, L. R. Watkins and S. F. Maier (2016). "The danger-
599 associated molecular pattern HMGB1 mediates the neuroinflammatory effects of methamphetamine." Brain
600 Behav Immun **51**: 99-108.
601 Goncalves, J., S. Baptista, T. Martins, N. Milhazes, F. Borges, C. F. Ribeiro, J. O. Malva and A. P. Silva
602 (2010). "Methamphetamine-induced neuroinflammation and neuronal dysfunction in the mice hippocampus:
603 preventive effect of indomethacin." Eur J Neurosci **31**(2): 315-326.
604 Goncalves, J., R. A. Leitao, A. Higuera-Matas, M. A. Assis, S. M. Coria, C. Fontes-Ribeiro, E. Ambrosio and
605 A. P. Silva (2017). "Extended-access methamphetamine self-administration elicits neuroinflammatory
606 response along with blood-brain barrier breakdown." Brain Behav Immun **62**: 306-317.
607 Gonzales, R., L. Mooney and R. A. Rawson (2010). "The methamphetamine problem in the United States."
608 Annu Rev Public Health **31**: 385-398.

609 Gonzalez, B., S. Jayanthi, N. Gomez, O. V. Torres, M. H. Sosa, A. Bernardi, F. J. Urbano, E. Garcia-Rill, J.
610 L. Cadet and V. Bisagno (2018). "Repeated methamphetamine and modafinil induce differential cognitive
611 effects and specific histone acetylation and DNA methylation profiles in the mouse medial prefrontal cortex."
612 Prog Neuropsychopharmacol Biol Psychiatry **82**: 1-11.
613 Hickman, S. E., N. D. Kingery, T. K. Ohsumi, M. L. Borowsky, L. C. Wang, T. K. Means and J. El Khoury
614 (2013). "The microglial sensome revealed by direct RNA sequencing." Nat Neurosci **16**(12): 1896-1905.
615 Huang, M., E. Malovic, A. Ealy, H. Jin, V. Anantharam, A. Kanthasamy and A. G. Kanthasamy (2023).
616 "Microglial immune regulation by epigenetic reprogramming through histone H3K27 acetylation in
617 neuroinflammation." Front Immunol **14**: 1052925.
618 Jayanthi, S., A. P. Daiwile and J. L. Cadet (2021). "Neurotoxicity of methamphetamine: Main effects and
619 mechanisms." Exp Neurol **344**: 113795.
620 Kaikkonen, M. U., N. J. Spann, S. Heinz, C. E. Romanoski, K. A. Allison, J. D. Stender, H. B. Chun, D. F.
621 Tough, R. K. Prinjha, C. Benner and C. K. Glass (2013). "Remodeling of the enhancer landscape during
622 macrophage activation is coupled to enhancer transcription." Mol Cell **51**(3): 310-325.
623 Karila, L., A. Weinstein, H. J. Aubin, A. Benyamina, M. Reynaud and S. L. Batki (2010). "Pharmacological
624 approaches to methamphetamine dependence: a focused review." Br J Clin Pharmacol **69**(6): 578-592.
625 Kays, J. S. and B. K. Yamamoto (2019). "Evaluation of Microglia/Macrophage Cells from Rat Striatum and
626 Prefrontal Cortex Reveals Differential Expression of Inflammatory-Related mRNA after Methamphetamine."
627 Brain Sci **9**(12).
628 Kearns, A. M., B. M. Siemsen, J. L. Hopkins, R. A. Weber, M. D. Scofield, J. Peters and C. M. Reichel (2022).
629 "Chemogenetic inhibition of corticostriatal circuits reduces cued reinstatement of methamphetamine
630 seeking." Addict Biol **27**(1): e13097.
631 Keren-Shaul, H., A. Spinrad, A. Weiner, O. Matcovitch-Natan, R. Dvir-Szternfeld, T. K. Ulland, E. David, K.
632 Baruch, D. Lara-Astaiso, B. Toth, S. Itzkovitz, M. Colonna, M. Schwartz and I. Amit (2017). "A Unique
633 Microglia Type Associated with Restricting Development of Alzheimer's Disease." Cell **169**(7): 1276-1290
634 e1217.
635 Kitamura, O., T. Takeichi, E. L. Wang, I. Tokunaga, A. Ishigami and S. Kubo (2010). "Microglial and astrocytic
636 changes in the striatum of methamphetamine abusers." Leg Med (Tokyo) **12**(2): 57-62.

637 Kiyatkin, E. A. and H. S. Sharma (2011). "Expression of heat shock protein (HSP 72 kDa) during acute
638 methamphetamine intoxication depends on brain hyperthermia: neurotoxicity or neuroprotection?" J Neural
639 Transm (Vienna) **118**(1): 47-60.
640 Krasnova, I. N., Z. Justinova and J. L. Cadet (2016). "Methamphetamine addiction: involvement of CREB
641 and neuroinflammatory signaling pathways." Psychopharmacology (Berl) **233**(10): 1945-1962.
642 Kuhn, D. M., D. M. Francescutti-Verbeem and D. M. Thomas (2006). "Dopamine quinones activate microglia
643 and induce a neurotoxic gene expression profile: relationship to methamphetamine-induced nerve ending
644 damage." Ann N Y Acad Sci **1074**: 31-41.
645 LaVoie, M. J., J. P. Card and T. G. Hastings (2004). "Microglial activation precedes dopamine terminal
646 pathology in methamphetamine-induced neurotoxicity." Exp Neurol **187**(1): 47-57.
647 Li, X., F. J. Rubio, T. Zeric, J. M. Bossert, S. Kambhampati, H. M. Cates, P. J. Kennedy, Q. R. Liu, R. Cimbro,
648 B. T. Hope, E. J. Nestler and Y. Shaham (2015). "Incubation of methamphetamine craving is associated with
649 selective increases in expression of Bdnf and trkb, glutamate receptors, and epigenetic enzymes in cue-
650 activated fos-expressing dorsal striatal neurons." J Neurosci **35**(21): 8232-8244.
651 Liao, L. S., S. Lu, W. T. Yan, S. C. Wang, L. M. Guo, Y. D. Yang, K. Huang, X. M. Hu, Q. Zhang, J. Yan and
652 K. Xiong (2021). "The Role of HSP90alpha in Methamphetamine/Hyperthermia-Induced Necroptosis in Rat
653 Striatal Neurons." Front Pharmacol **12**: 716394.
654 Limanaqi, F., S. Gambardella, F. Biagioni, C. L. Busceti and F. Fornai (2018). "Epigenetic Effects Induced by
655 Methamphetamine and Methamphetamine-Dependent Oxidative Stress." Oxid Med Cell Longev **2018**:
656 4982453.
657 Mark, K. A., J. J. Soghomonian and B. K. Yamamoto (2004). "High-dose methamphetamine acutely activates
658 the striatonigral pathway to increase striatal glutamate and mediate long-term dopamine toxicity." J Neurosci
659 **24**(50): 11449-11456.
660 Masuda, T., R. Sankowski, O. Staszewski, C. Bottcher, L. Amann, Sagar, C. Scheiwe, S. Nessler, P. Kunz,
661 G. van Loo, V. A. Coenen, P. C. Reinacher, A. Michel, U. Sure, R. Gold, D. Grun, J. Priller, C. Stadelmann
662 and M. Prinz (2019). "Spatial and temporal heterogeneity of mouse and human microglia at single-cell
663 resolution." Nature **566**(7744): 388-392.

664 Matcovitch-Natan, O., D. R. Winter, A. Giladi, S. Vargas Aguilar, A. Spinrad, S. Sarrazin, H. Ben-Yehuda, E.
665 David, F. Zelada Gonzalez, P. Perrin, H. Keren-Shaul, M. Gury, D. Lara-Astaiso, C. A. Thaiss, M. Cohen, K.
666 Bahar Halpern, K. Baruch, A. Deczkowska, E. Lorenzo-Vivas, S. Itzkovitz, E. Elinav, M. H. Sieweke, M.
667 Schwartz and I. Amit (2016). "Microglia development follows a stepwise program to regulate brain
668 homeostasis." Science **353**(6301): aad8670.
669 McCarthy, M. M., B. M. Nugent and K. M. Lenz (2017). "Neuroimmunology and neuroepigenetics in the
670 establishment of sex differences in the brain." Nat Rev Neurosci **18**(8): 471-484.
671 McConnell, S. E., M. K. O'Banion, D. A. Cory-Slechta, J. A. Olschowka and L. A. Opanashuk (2015).
672 "Characterization of binge-dosed methamphetamine-induced neurotoxicity and neuroinflammation."
673 Neurotoxicology **50**: 131-141.
674 McHugh, R. K., V. R. Votaw, D. E. Sugarman and S. F. Greenfield (2018). "Sex and gender differences in
675 substance use disorders." Clin Psychol Rev **66**: 12-23.
676 Meleady, L., M. Towriss, J. Kim, V. Bacarac, V. Dang, M. E. Rowland and A. V. Ciernia (2023). "Histone
677 deacetylase 3 regulates microglial function through histone deacetylation." Epigenetics **18**(1): 2241008.
678 Morrison, H., K. Young, M. Qureshi, R. K. Rowe and J. Lifshitz (2017). "Quantitative microglia analyses reveal
679 diverse morphologic responses in the rat cortex after diffuse brain injury." Sci Rep **7**(1): 13211.
680 Nicosia, N., R. L. Pacula, B. Kilmer, R. Lundberg and J. Chiesa (2009). "The Economic Cost of
681 Methamphetamine Use in the United States, 2005." RAND Corporation.
682 Omonijo, O., P. Wongprayoon, B. Ladenheim, M. T. McCoy, P. Govitrapong, S. Jayanthi and J. L. Cadet
683 (2014). "Differential effects of binge methamphetamine injections on the mRNA expression of histone
684 deacetylases (HDACs) in the rat striatum." Neurotoxicology **45**: 178-184.
685 Osborne, B. F., A. Turano and J. M. Schwarz (2018). "Sex Differences in the Neuroimmune System." Curr
686 Opin Behav Sci **23**: 118-123.
687 Ostuni, R., V. Piccolo, I. Barozzi, S. Polletti, A. Termanini, S. Bonifacio, A. Curina, E. Prosperini, S. Ghisletti
688 and G. Natoli (2013). "Latent enhancers activated by stimulation in differentiated cells." Cell **152**(1-2): 157-
689 171.

690 Paolicelli, R. C., G. Bolasco, F. Pagani, L. Maggi, M. Scianni, P. Panzanelli, M. Giustetto, T. A. Ferreira, E.
691 Guiducci, L. Dumas, D. Ragozzino and C. T. Gross (2011). "Synaptic pruning by microglia is necessary for
692 normal brain development." Science **333**(6048): 1456-1458.
693 Parkhurst, C. N., G. Yang, I. Ninan, J. N. Savas, J. R. Yates, 3rd, J. J. Lafaille, B. L. Hempstead, D. R. Littman
694 and W. B. Gan (2013). "Microglia promote learning-dependent synapse formation through brain-derived
695 neurotrophic factor." Cell **155**(7): 1596-1609.
696 Robson, M. J., R. C. Turner, Z. J. Naser, C. R. McCurdy, J. D. Huber and R. R. Matsumoto (2013). "SN79, a
697 sigma receptor ligand, blocks methamphetamine-induced microglial activation and cytokine upregulation."
698 Exp Neurol **247**: 134-142.
699 Salter, M. W. and B. Stevens (2017). "Microglia emerge as central players in brain disease." Nat Med **23**(9):
700 1018-1027.
701 Savage, J. C., M. Carrier and M. E. Tremblay (2019). "Morphology of Microglia Across Contexts of Health
702 and Disease." Methods Mol Biol **2034**: 13-26.
703 Schindelin, J., I. Arganda-Carreras, E. Frise, V. Kaynig, M. Longair, T. Pietzsch, S. Preibisch, C. Rueden, S.
704 Saalfeld, B. Schmid, J. Y. Tinevez, D. J. White, V. Hartenstein, K. Eliceiri, P. Tomancak and A. Cardona
705 (2012). "Fiji: an open-source platform for biological-image analysis." Nat Methods **9**(7): 676-682.
706 Schwarz, J. M., M. R. Hutchinson and S. D. Bilbo (2011). "Early-life experience decreases drug-induced
707 reinstatement of morphine CPP in adulthood via microglial-specific epigenetic programming of anti-
708 inflammatory IL-10 expression." J Neurosci **31**(49): 17835-17847.
709 Sekine, Y., Y. Ouchi, G. Sugihara, N. Takei, E. Yoshikawa, K. Nakamura, Y. Iwata, K. J. Tsuchiya, S. Suda,
710 K. Suzuki, M. Kawai, K. Takebayashi, S. Yamamoto, H. Matsuzaki, T. Ueki, N. Mori, M. S. Gold and J. L.
711 Cadet (2008). "Methamphetamine causes microglial activation in the brains of human abusers." J Neurosci
712 **28**(22): 5756-5761.
713 Sholl, D. A. (1953). "Dendritic organization in the neurons of the visual and motor cortices of the cat." J Anat
714 **87**(4): 387-406.
715 Spangenberg, E., P. L. Severson, L. A. Hohsfield, J. Crapser, J. Zhang, E. A. Burton, Y. Zhang, W. Spevak,
716 J. Lin, N. Y. Phan, G. Habets, A. Rymar, G. Tsang, J. Walters, M. Nespi, P. Singh, S. Broome, P. Ibrahim, C.

717 Zhang, G. Bollag, B. L. West and K. N. Green (2019). "Sustained microglial depletion with CSF1R inhibitor
718 impairs parenchymal plaque development in an Alzheimer's disease model." Nat Commun **10**(1): 3758.
719 Starossom, S. C., I. D. Mascanfroni, J. Imitola, L. Cao, K. Raddassi, S. F. Hernandez, R. Bassil, D. O. Croci,
720 J. P. Cerliani, D. Delacour, Y. Wang, W. Elyaman, S. J. Khoury and G. A. Rabinovich (2012). "Galectin-1
721 deactivates classically activated microglia and protects from inflammation-induced neurodegeneration."
722 Immunity **37**(2): 249-263.
723 Stolero, N. and D. Frenkel (2021). "The dialog between neurons and microglia in Alzheimer's disease: The
724 neurotransmitters view." J Neurochem **158**(6): 1412-1424.
725 Takashima, Y., M. J. Fannon, M. H. Galinato, N. L. Steiner, M. An, A. E. Zemljic-Harpf, S. S. Somkuwar, B. P.
726 Head and C. D. Mandyam (2018). "Neuroadaptations in the dentate gyrus following contextual cued
727 reinstatement of methamphetamine seeking." Brain Struct Funct **223**(5): 2197-2211.
728 Thanos, P. K., R. Kim, F. Delis, M. Ananth, G. Chachati, M. J. Rocco, I. Masad, J. A. Muniz, S. C. Grant, M.
729 S. Gold, J. L. Cadet and N. D. Volkow (2016). "Chronic Methamphetamine Effects on Brain Structure and
730 Function in Rats." PLoS One **11**(6): e0155457.
731 Theberge, F. R., X. Li, S. Kambhampati, C. L. Pickens, R. St Laurent, J. M. Bossert, M. H. Baumann, M. R.
732 Hutchinson, K. C. Rice, L. R. Watkins and Y. Shaham (2013). "Effect of chronic delivery of the Toll-like
733 receptor 4 antagonist (+)-naltrexone on incubation of heroin craving." Biol Psychiatry **73**(8): 729-737.
734 Thomas, D. M., P. D. Walker, J. A. Benjamins, T. J. Geddes and D. M. Kuhn (2004). "Methamphetamine
735 neurotoxicity in dopamine nerve endings of the striatum is associated with microglial activation." J Pharmacol
736 Exp Ther **311**(1): 1-7.
737 van Landeghem, F. K., J. F. Stover, I. Bechmann, W. Bruck, A. Unterberg, C. Buhrer and A. von Deimling
738 (2001). "Early expression of glutamate transporter proteins in ramified microglia after controlled cortical
739 impact injury in the rat." Glia **35**(3): 167-179.
740 Vidal-Itriago, A., R. A. W. Radford, J. A. Aramideh, C. Maurel, N. M. Scherer, E. K. Don, A. Lee, R. S. Chung,
741 M. B. Graeber and M. Morsch (2022). "Microglia morphophysiological diversity and its implications for the
742 CNS." Front Immunol **13**: 997786.
743 Vilca, S. J., A. V. Margetts, T. A. Pollock and L. M. Tuesta (2023). "Transcriptional and epigenetic regulation
744 of microglia in substance use disorders." Mol Cell Neurosci **125**: 103838.

745 Wake, H., A. J. Moorhouse, A. Miyamoto and J. Nabekura (2013). "Microglia: actively surveying and shaping
746 neuronal circuit structure and function." Trends Neurosci **36**(4): 209-217.
747 Wang, X., A. L. Northcutt, T. A. Cochran, X. Zhang, T. J. Fabisiak, M. E. Haas, J. Amat, H. Li, K. C. Rice, S.
748 F. Maier, R. K. Bachtell, M. R. Hutchinson and L. R. Watkins (2019). "Methamphetamine Activates Toll-Like
749 Receptor 4 to Induce Central Immune Signaling within the Ventral Tegmental Area and Contributes to
750 Extracellular Dopamine Increase in the Nucleus Accumbens Shell." ACS Chem Neurosci **10**(8): 3622-3634.
751 Wydra, K., K. Golembiowska, M. Zaniewska, K. Kaminska, L. Ferraro, K. Fuxe and M. Filip (2013). "Accumbal
752 and pallidal dopamine, glutamate and GABA overflow during cocaine self-administration and its extinction in
753 rats." Addict Biol **18**(2): 307-324.
754 Yan, Y., A. Nitta, T. Koseki, K. Yamada and T. Nabeshima (2012). "Dissociable role of tumor necrosis factor
755 alpha gene deletion in methamphetamine self-administration and cue-induced relapsing behavior in mice."
756 Psychopharmacology (Berl) **221**(3): 427-436.
757 Yang, X., Y. Wang, Q. Li, Y. Zhong, L. Chen, Y. Du, J. He, L. Liao, K. Xiong, C. X. Yi and J. Yan (2018). "The
758 Main Molecular Mechanisms Underlying Methamphetamine- Induced Neurotoxicity and Implications for
759 Pharmacological Treatment." Front Mol Neurosci **11**: 186.
760 Yeh, H. and T. Ikezu (2019). "Transcriptional and Epigenetic Regulation of Microglia in Health and Disease."
761 Trends Mol Med **25**(2): 96-111.
762 Yu, Z., W. Chen, L. Zhang, Y. Chen, W. Chen, S. Meng, L. Lu, Y. Han and J. Shi (2023). "Gut-derived bacterial
763 LPS attenuates incubation of methamphetamine craving via modulating microglia." Brain Behav Immun **111**:
764 101-115.
765

766 **Supplementary Methods and Results**

767

768 **RNA-sequencing analysis of isolated striatal microglia.**

769 Biological replicates determined to be outliers were removed for differential gene expression analysis
770 (**Supplementary Fig. 1A**). Principal component analysis (PCA) (**Supplementary Fig. 1B**) and heatmap of
771 hierarchical clustering of conditions based on gene expression (**Supplementary Fig. 1C**) shows high
772 similarity of samples within condition, and that animals exposed to methamphetamine (Maintenance and
773 Abstinence) cluster more closely than to Saline.

774

775 **Microglia are not required for natural food reinforcement.**

776 To test if microglia are necessary for learned operant behavior, we food-trained mice up to FR5 for 8
777 consecutive days (**Supplementary Fig. 2**). Mice were treated with PLX5622 (1200 ppm in AIN-76A chow)
778 for the duration of the experiment. Microglial ablation does not affect natural food reinforcement in number
779 of rewards earned (**Supplementary Fig. 2A**) (Two-way RM ANOVA; AIN-76A vs PLX5622, $F(1, 13) =$
780 0.07321, $p=0.7910$) or lever discrimination (**Supplementary Fig. 2B**) (Two-way RM ANOVA; Active vs
781 Inactive Lever, $F(3, 26) = 24.38$, $p<0.0001$) and time to acquire operant lever pressing behavior
782 (**Supplementary Fig. 2B**) (Two-way RM ANOVA; AIN-76A vs PLX5622, $F(1, 13) = 0.3855$, $p=0.5454$).

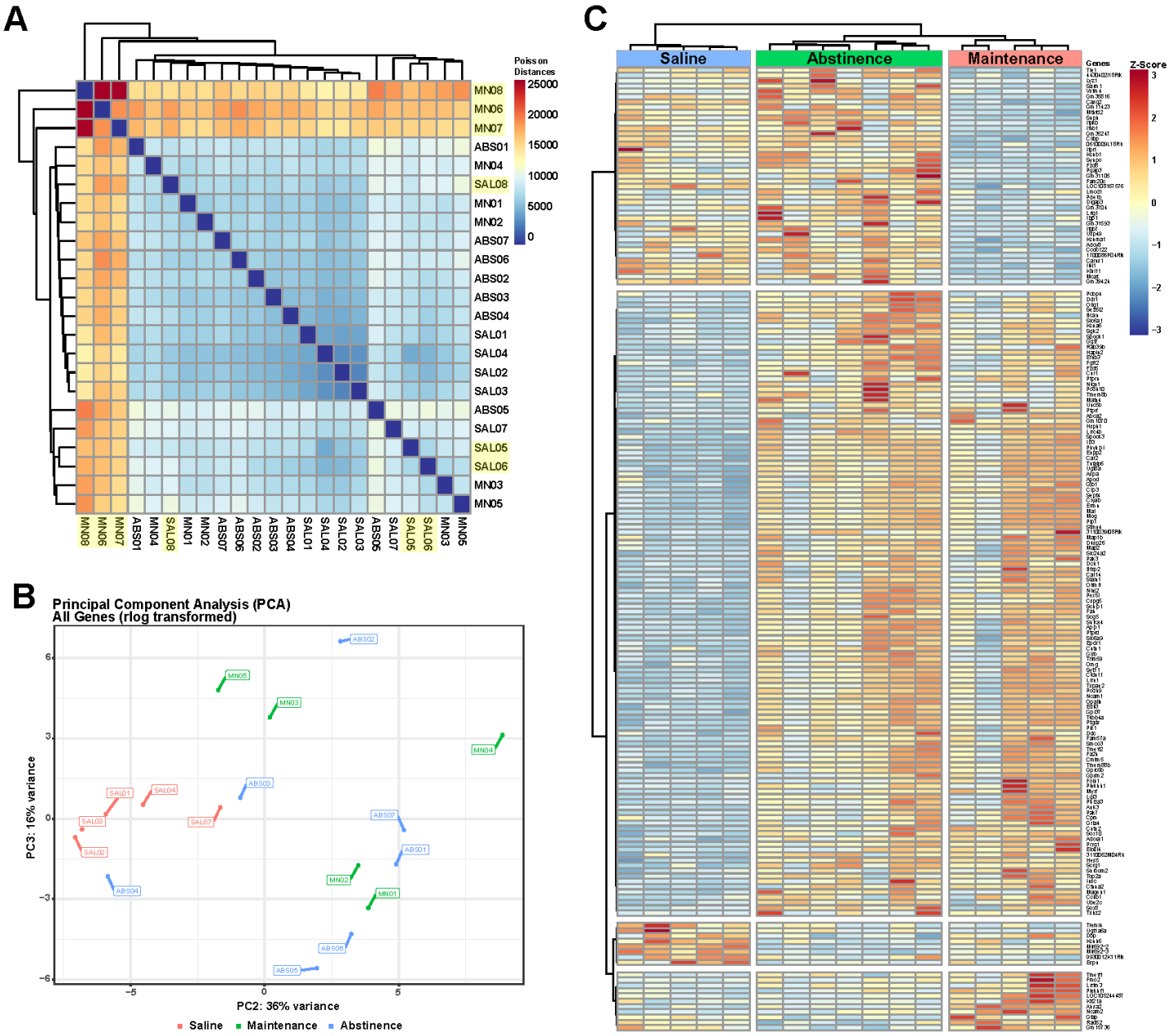

783
784

785 **Supplementary Figure 1. RNA-sequencing of isolated striatal microglia from METH IVSA. A)**
786 Hierarchical clustering heatmap of expression profiles for samples (n=23) based on Poisson distance.
787 Highlighted samples were determined to be outliers and were removed from analyses. **B)** PCA plot for
788 samples (n=17) following removal of outliers. **C)** Heatmap showing unsupervised clustering of samples based
789 on gene expression.

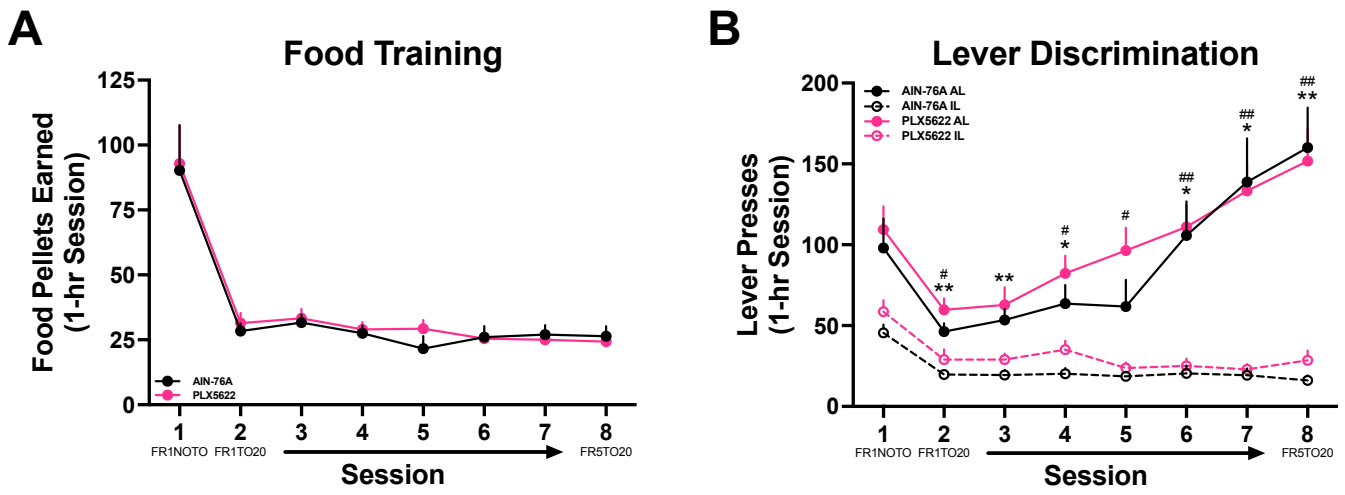

Supplementary Figure 2. Pharmacological ablation of microglia does not affect operant responding. **A)** Number of food rewards earned during 8 daily 1-hr sessions. **(B)** Active vs inactive lever presses during 8 daily 1-hr sessions (Two-way RM ANOVA with Bonferroni post-hoc test; AIN-76A Active vs Inactive Lever, *$p < 0.05$, **$p < 0.01$; PLX5622 Active vs Inactive Lever, $^{\#}p < 0.05$, $^{\#\#}p < 0.01$). AIN-76A (n=8), PLX5622 (n=7). Data are represented as mean ± SEM.

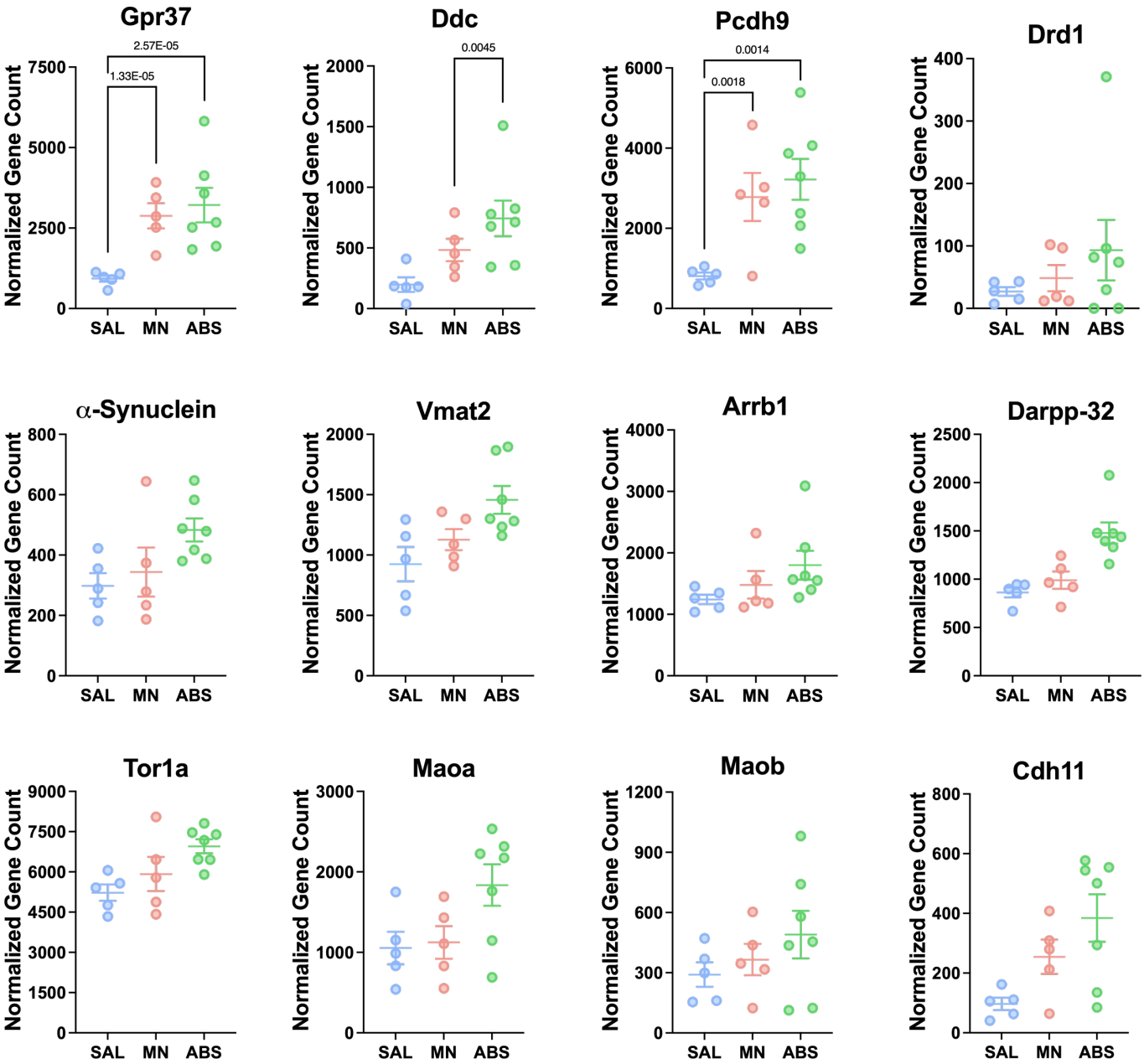

Supplementary Figure 3. Dopamine signaling-related genes. Normalized counts of DE genes with adjusted p-value for each comparison.

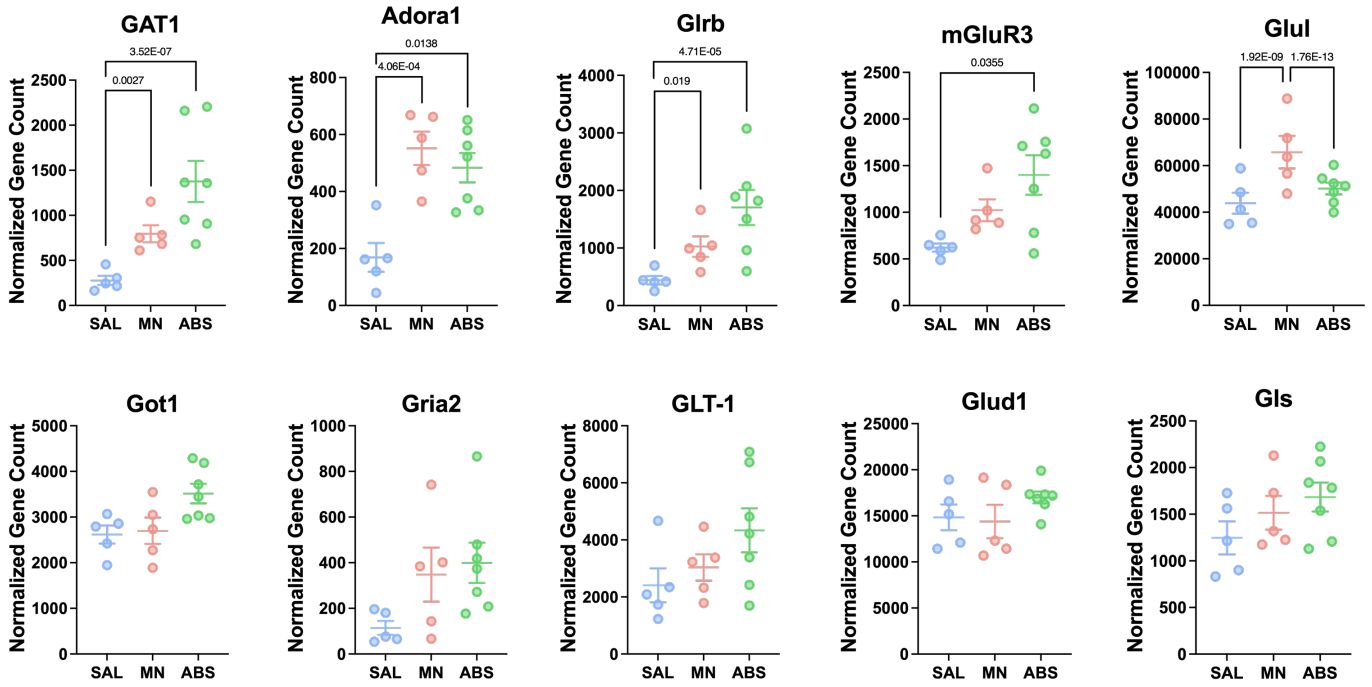

Supplementary Figure 4. GABA, glutamate and adenosine signaling-related genes. Normalized counts of DE genes related to GABA, glutamate, and adenosine signaling with adjusted p-value for each comparison.